Linear Layouts of Bipartite Planar Graphs

Henry Förster
Department of Computer Science, University of Tübingen, Tübingen, Germany

Michael Kaufmann
Department of Computer Science, University of Tübingen, Tübingen, Germany

Laura Merker
Institute of Theoretical Informatics, Karlsruhe Institute of Technology, Germany

Sergey Pupyrev
Meta Platforms Inc., Menlo Park, CA, USA

Chrysanthi N. Raftopoulou
National Technical University of Athens, Greece

Abstract

A linear layout of a graph G consists of a linear order $\prec$ of the vertices and a partition of the edges. A part is called a *queue* (*stack*) if no two edges nest (cross), that is, two edges (v, w) and (x, y) with $v \prec x \prec y \prec w$ ($v \prec x \prec w \prec y$) may not be in the same queue (stack). The best known lower and upper bounds for the number of queues needed for planar graphs are 4 [Alam et al., Algorithmica 2020] and 42 [Bekos et al., Algorithmica 2022], respectively. While queue layouts of special classes of planar graphs have received increased attention following the breakthrough result of [Dujmović et al., J. ACM 2020], the meaningful class of bipartite planar graphs has remained elusive so far, explicitly asked for by Bekos et al. In this paper we investigate bipartite planar graphs and give an improved upper bound of 28 by refining existing techniques. In contrast, we show that two queues or one queue together with one stack do not suffice; the latter answers an open question by Pupyrev [GD 2018]. We further investigate subclasses of bipartite planar graphs and give improved upper bounds; in particular we construct 5-queue layouts for 2-degenerate quadrangulations.

Keywords and phrases bipartite planar graphs, queue number, mixed linear layouts, graph product structure

Related Version An extended abstract of this paper appears in the Proceedings of the 18th International Symposium on Algorithms and Data Structures, WADS 2023

Acknowledgements This research was initiated at the GNV workshop in Heiligkreuztal, Germany, June 26 – July 1, 2022, organized by Michalis Bekos and Michael Kaufmann. Thanks to the organizers and other participants for creating a productive environment.

1 Introduction

Since the 1980s, linear graph layouts have been a central combinatorial problem in topological graph theory, with a wealth of publications [7, 8, 12, 17, 20, 21, 22, 26, 27, 36]. A *linear layout* of a graph consists of a linear order $\prec$ of the vertices and a partition of the edges into *stacks* and *queues*. A part is called a *queue* (*stack*) if no two edges of this part nest (cross), that is, two edges (v, w) and (x, y) with $v \prec x \prec y \prec w$ ($v \prec x \prec w \prec y$) may not be in the same queue (stack). Most notably, research has focused on so-called *stack layouts* (also known as book-embeddings) and *queue layouts* where either all parts are *stacks* or all parts are *queues*, respectively. While these kinds of graph layouts appear quite restrictive on first sight, they are in fact quite important in practice. For instance, stack layouts are used as a model for chip design [17], while queue layouts find applications in three-dimensional network visualization [14, 22, 24]. For these applications, it is important that the edges are partitioned into as few stacks or queues as possible. This notion is captured by the *stack* *number*, $\mathrm{sn}(G)$, and *queue number*, $\mathrm{qn}(G)$, of a graph G, which denote how many stacks or queues are required in a stack and a queue layout of G, respectively. Similarly, *mixed linear layouts*, where both stacks and queues are allowed, have emerged as a research direction in the past few years [3, 18, 31].

Recently, queue layouts have received much attention as several breakthroughs were made which pushed the field further. Introduced in 1992 [27], it was conjectured in the same year [26], that all planar graphs have a bounded queue number. Despite various attempts at settling the conjecture [5, 6, 10, 20], it remained unanswered for almost 30 years. In 2019, the conjecture was finally affirmed by Dujmović, Joret, Micek, Morin, Ueckerdt and Wood [21]. Their proof relies on three ingredients: First, it was already known that graphs of bounded treewidth have bounded queue number [34]. Second, they showed that the *strong product* of a graph of bounded queue number and a path has bounded queue number. Finally, and most importantly, they proved that every planar graph is a subgraph of the *strong product* of a path and a graph of treewidth at most 8. In the few years following the result, both queue layouts [1, 7, 13, 19, 28] and graph product structure [9, 15, 16, 29, 33, 35] have become important research directions. Yet, after all recent developments, the best known upper bound for the queue number of planar graphs is 42 [7] whereas the best known corresponding lower bound is 4 [2]. This stands in contrast to a tight bound of 4 for the stack number of planar graphs [11, 36].

It is noteworthy that better upper bounds of the queue number are known only for certain subclasses of planar graphs, such as planar 3-trees [2] and posets [1], or for relaxed variants of the queue number [28]. It remains elusive how other properties of a graph, such as a bounded degree or bipartiteness, can be used to reduce the gap between the lower and the upper bounds on the queue number; see also the open problems raised in [7] which contains the currently best upper bound. This is partially due to the fact that it is not well understood how these properties translate into the product structure of the associated graph classes. In fact, the product structure theorem has been improved for general planar graphs [33] while, to the best of our knowledge, there are very few results that yield stronger properties for subclasses thereof. Here, we contribute to this line of research by studying bipartite planar graphs.

Results. Our paper focuses on the queue number of bipartite graphs and subclasses thereof. We start by revisiting results from the existing literature in Section 2. In particular, we discuss techniques that are used to bound the queue number of general planar graphs by 42 [7, 21] and refine them to obtain an improved upper bound on the queue number of bipartite planar graphs.

▸ **Theorem 1.** *The queue number of bipartite planar graphs is at most* 28.

We then improve this bound for interesting subfamilies of bipartite planar graphs. For this we first prove a product structure theorem for stacked quadrangulations, which is a family of graphs that may be regarded as a bipartite variant of planar 3-trees. We remark that we avoid the path factor that is present in most known product structure theorems.

▸ **Theorem 2.** *Every stacked quadrangulation is a subgraph of $H \boxtimes C_4$, where H is a planar* 3*-tree.*

In fact, our result generalizes to similarly constructed graph classes. Based on Theorem 2, we improve the upper bound on the queue number of stacked quadrangulations.

▸ **Theorem 3.** *The queue number of stacked quadrangulations is at most* 21.

Complementing our upper bounds, we provide lower bounds on the queue number and the mixed page number of bipartite planar graphs in Section 4. Both results improve the state-of-the-art for bipartite planar graphs, while additionally providing a lower bound for the special case of 2-degenerate bipartite planar graphs. We remark that Theorem 5 answers a question asked in [3, 18, 31].

▸ **Theorem 4.** *There is a* 2*-degenerate bipartite planar graph with queue number at least* 3*.*

▸ **Theorem 5.** *There is a* 2*-degenerate bipartite planar graph that does not admit a* 1*-queue* 1*-stack layout.*

For this purpose, we use a family of 2-degenerate quadrangulations. Finally, inspired by our lower bound construction, we conclude with investigating this graph class.

▸ **Theorem 6.** *Every* 2*-degenerate quadrangulation admits a* 5*-queue layout.*

Outline. We start with basic results on the queue number of bipartite planar graphs in Section 2, where we prove Theorem 1. Section 3 provides a definition of stacked quadrangulations and an investigation of their structure including proofs of Theorems 2 and 3. We continue with lower bounds in Section 4 and then further investigate the graphs constructed there in Section 5, in particular we prove Theorem 6.

2 Preliminaries

In this section, we introduce basic definitions and tools that we use to analyze the queue number of bipartite planar graphs and refine them to prove Theorem 1.

2.1 Definitions

Classes of bipartite planar graphs. In this paper, we study subclasses of *planar* graphs, that is graphs admitting a *planar drawing*. A special type of planar drawings are *leveled planar drawings* where the vertices are placed on a sequence of parallel lines (levels) and every edge joins vertices in two consecutive levels. We call a graph *leveled planar* if it admits a leveled planar drawing.

A planar drawing partitions the plane into regions called *faces*. It is well known that the *maximal* planar graphs, that is, the planar graphs to which no crossing-free edge can be added, are exactly the triangulations of the plane, that is, every face is a triangle. We focus on the *maximal bipartite planar graphs* which are exactly the quadrangulations of the plane, that is, every face is a quadrangle. In the following, we introduce interesting families of quadrangulations.

One such family are the *stacked quadrangulations* that can be constructed as follows. First, a square is a stacked quadrangulation. Second, if G is a stacked quadrangulation and f is a face of G, then inserting a plane square S into f and connecting the four vertices of S with a planar matching to the four vertices of f again yields a stacked quadrangulation. Note that every face has four vertices, that is, the constructed graph is indeed a quadrangulation. We are particularly interested in this family of quadrangulations as stacked quadrangulations can be regarded as the bipartite variant of the well-known graph class *planar* 3*-trees* which are also known as *stacked triangulations*. This class again can be recursively defined as follows: A *planar* 3*-tree* is either a triangle or a graph that can be obtained from a planar 3-tree by adding a vertex v into some face f and connecting v to the three vertices of f. This class is particularly interesting in the context of queue layouts as it provides the currently best lower bound on the queue number of planar graphs [2].

The notions of stacked triangulations and stacked quadrangulations can be generalized as follows using once again a recursive definition. For $t \geqslant 3$ and $s \geqslant 1$, any connected planar graph of order at most s is called a (t, s)-stacked graph. Moreover, for a (t, s)-stacked graph G and a connected planar graph G' with at most s vertices, we obtain another (t, s)-stacked graph G'' by connecting G' to the vertices of a face f of G in a planar way such that each face of G'' has at most t vertices. Note that we do not require that the initial graph G and the connected stacked graph G' of order at most s in the recursive definition have only faces of size at most t as this will not be required by our results in Section 3. If in each recursive step the edges between G' and the vertices of f form a matching, then the resulting graph is called an *(t, s)-matching-stacked graph*. Now, in particular $(3, 1)$-stacked graphs are the planar 3-trees while the stacked quadrangulations are a subclass of the $(4, 4)$-matching-stacked graphs. In addition, $(3, 3)$-stacked graphs are the *stacked octahedrons*, which were successfully used to construct planar graphs that require four stacks [11, 37].

In addition to graphs obtained by recursive stacking operations, we will also study graphs that are restricted by *degeneracy*. Namely, we call a graph $G = (V, E)$ d-degenerate if there exists a total order $(v_1, \dots, v_n)$ of V, so that for $1 \leqslant i \leqslant n$, v_i has degree at most d in the subgraph induced by vertices $(v_1, \dots, v_i)$. Of particular interest will be a family of 2-degenerate quadrangulations discussed in Section 4. It is worth pointing out that there are recursive constructions for triconnected and simple quadrangulations that use the insertion of degree-2 vertices and $(4, 4)$-matching stacking in their iterative steps [25].

Linear layouts. A *linear layout* of a graph $G = (V, E)$ consists of an order $\prec$ of V and a partition $\mathcal{P}$ of E. Consider two disjoint edges $(v, w), (x, y) \in E$. We say that (v, w) *nests* (x, y) if $v \prec x \prec y \prec w$, and we say that (v, w) and (x, y) *cross* if $v \prec x \prec w \prec y$. For each part $P \in \mathcal{P}$ we require that either no two edges of P nest or that no two edges of P cross. We call P a *queue* in the former and a *stack* in the latter case. Let $\mathcal{Q} \subseteq \mathcal{P}$ denote the set of queues and let $\mathcal{S} \subseteq \mathcal{P}$ denote the set of stacks; such a linear layout is referred to as a $|\mathcal{Q}|$-*queue* $|\mathcal{S}|$-*stack* layout. If $\mathcal{Q} \neq \emptyset$ and $\mathcal{S} \neq \emptyset$, we say that the linear layout is *mixed*, while when $\mathcal{S} = \emptyset$, it is called a $|\mathcal{Q}|$-*queue* layout. The *queue number*, $\mathrm{qn}(G)$, of a graph G is the minimum value q such that G admits a q-queue layout. Heath and Rosenberg [27] characterize graphs admitting a 1-queue layout in terms of *arched-leveled* layouts. In particular, this implies that each *leveled planar graph* admits a 1-queue layout. Indeed a bipartite graph has queue number 1 if and only if it is leveled planar [4].

In the remainder of this subsection, we define important tools that have been used in the context of linear layouts in the past and also are essential in our proofs.

Important tools. The *strong product* $G_1 \boxtimes G_2$ of two graphs G_1 and G_2 is a graph with vertex set $V(G_1) \times V(G_2)$ and an edge between two vertices (v_1, v_2) and (w_1, w_2) if (i) $v_1 = w_1$ and $(v_2, w_2) \in E(G_2)$, (ii) $v_2 = w_2$ and $(v_1, w_1) \in E(G_1)$, or (iii) $(v_1, w_1) \in E(G_1)$ and $(v_2, w_2) \in E(G_2)$.

Given a graph G, an *H-partition* of G is a pair $\big(H, \{V_x : x \in V(H)\}\big)$ consisting of a graph H and a partition of V into sets $\{V_x : x \in V(H)\}$ called *bags* such that for every edge $(u, v) \in E$ one of the following holds: (i) $u, v \in V_x$ for some $x \in V(H)$, or (ii) there is an edge (x, y) of H with $u \in V_x$ and $v \in V_y$. In Case (i), we call (u, v) an *intra-bag* edge, while we call it *inter-bag* in Case (ii). To avoid confusion with the vertices of G, the vertices of H are called *nodes*. The *width* of an H-partition is defined as the maximum size of a bag. It is easy to see that a graph G has an H-partition of width w if and only if it is a subgraph of $H \boxtimes K_w$ (compare Observation 35 of [21]). In the case where H is a tree, we call the H-partition a *tree-partition*. We refer to Figure 15 for an example of a tree-partition.

A related concept to H-partitions are *tree decompositions*. Given a graph G, a *tree decomposition* of G is a pair $\big(T, \{B_x : x \in V(T)\}\big)$ consisting of a tree T where every vertex $x \in V(T)$ is associated with a subset B_x, called *bag*, of the vertices of G so that the following hold: (i) $\bigcup_{x \in V(T)} B_x = V(G)$, (ii) for each $(u, v) \in E(G)$ there exists at least one bag B_x so that $u \in B_x$ and $v \in B_x$, and (iii) for every $v \in V(G)$, the set of nodes whose bags contain v induce a connected subtree of T. Observe that in contrast to a tree-partition, the bags are in general not disjoint. The *treewidth* of a tree decomposition is the cardinality of the largest bag minus one. Moreover, the *treewidth* of a graph is the minimum treewidth of any of its tree decompositions.

2.2 General Bipartite Planar Graphs

Following existing works on queue layouts of planar graphs, we get the following upper bound for the class of bipartite planar graphs.

▸ **Theorem 1.** *The queue number of bipartite planar graphs is at most* 28*.*

A key component of the state-of-the-art bounds on the queue number of planar graphs are H-partitions with low layered width. A *BFS-layering* of G is a partition of $V(G)$ into $\mathcal{L} = (V_0, V_1, \ldots)$ such that V_i contains exactly the vertices with graph-theoretic distance i from a specified vertex $r \in V(G)$. We refer to each V_i as a *layer*. We say that an H-partition $(H, \{A_x : x \in V(H)\})$ of a graph G has *layered-width* ℓ if and only if there is a BFS-layering $\mathcal{L} = (V_0, V_1, \ldots)$ of G so that for every $x \in V(H)$ and every i it holds that $|A_x \cap V_i| \leqslant \ell$. The following theorem plays an important role in computing queue layouts for planar graphs with a constant number of queues.

▷ Claim 7 (Theorem 15 of [21]). Every planar graph G has an H-partition with layered-width 3 such that H is planar and has treewidth at most 3. Moreover, there is such a partition for every BFS layering of G.

There are two noteworthy observations regarding Claim 7. First, for a bipartite planar graph with parts A and B so that $V = A \dot\cup B$, a BFS-layering $\mathcal{L} = (V_0, V_1, \ldots)$ is so that without loss of generality for every integer k, it holds $V_{2k} \cap B = \varnothing$ and $V_{2k+1} \cap A = \varnothing$. We will call such a layering *bichromatic* and we say that an H-partition $\{A_x | x \in V(H)\}$ of a bipartite graph G has *bichromatic layered-width* ℓ if and only if there is a bichromatic BFS-layering $\mathcal{L} = (V_0, V_1, \ldots)$ of G so that for every $x \in V(H)$ and every i it holds that $|A_x \cap V_i| \leqslant \ell$.

Second, on the other hand, the proof of Claim 7 assumes G to be triangulated. Hence, it is not immediate, that the following special case of Claim 7 is true:

▸ **Lemma 8.** *Every bipartite planar graph G has a H-partition with bichromatic layered-width* 3 *such that H is planar and has treewidth at most 3.*

Proof. We begin by quadrangulating the input graph G obtaining the quadrangulation G'. Then, we perform a BFS traversal of G'. In the resulting layering, every quadrangle $q = (a_1, b_1, a_2, b_2)$ is (up to relabeling) either such that $a_1 \in V_i$, $b_1, b_2, \in V_{i+1}$ and $a_2 \in V_{i+2}$ or such that $a_1, a_2 \in V_i$, $b_1, b_2, \in V_{i+1}$. In either case, we can triangulate q with edge (b_1, b_2). Applying this procedure to all quadrangles yields a triangulated supergraph G'' that has the property that the layering obtained from G' still is a valid layering for G''. Then, we can apply Claim 7 to obtain the H-partition for G'' which serves as the required bichromatic H-partition for graph G. ◂

Based on this decomposition, Dujmović et al. [21] compute a queue-layout using the following lemma:

▻ Claim 9 (Lemma 8 of [21]). For all graphs H and G, if H has a k-queue layout and G has an H-partition of layered-width ℓ with respect to some layering $(V_0, V_1, \dots)$ of G, then G has a $(3\ell k + \lfloor \frac{3}{2}\ell \rfloor)$-queue layout using vertex order $\overrightarrow{V_0}, \overrightarrow{V_1}, \dots$, where $\overrightarrow{V_i}$ is some order of V_i. In particular,

$$\mathrm{qn}(G) \leqslant 3\ell \ \mathrm{qn}(H) + \left\lfloor \frac{3}{2}\ell \right\rfloor. \tag{1}$$

In order to improve the lemma for bipartite planar graphs, we briefly sketch which components the upper bound of $\mathrm{qn}(G)$ in (1) is composed of.

Sketch of the proof of Claim 9. The main argument here, is to classify edges as *intra-bag* or *inter-bag* as well as as *intra-layer* or *inter-layer*. Namely, an edge is called *intra-bag* if its two endpoints occur in the same bag A_x with $x \in V(H)$. Otherwise, it is called *inter-bag*. Similarly, an edge is called *intra-layer* if both its endpoints occur on the same layer V_i, otherwise it is called *inter-layer*.

For each classification of edges, different queues are used. More precisely:

E.1 Intra-layer intra-bag edges may induce a K_ℓ, hence there are at most $\lfloor \frac{\ell}{2} \rfloor$ queues needed for such edges.

E.2 Inter-layer intra-bag edges may induce a $K_{\ell,\ell}$, hence there are at most ℓ queues needed for such edges.

E.3 Intra-layer inter-bag edges corresponding to the same edge of H may induce a $K_{\ell,\ell}$, hence there are at most ℓk queues needed for such edges as H has queue number at most k.

E.4 Inter-layer inter-bag *forward*[1] edges corresponding to the same edge of H may induce a $K_{\ell,\ell}$, hence there are at most ℓk queues needed for such edges as H has queue number at most k.

E.5 Inter-layer inter-bag *backward* edges corresponding to the same edge of H may induce a $K_{\ell,\ell}$, hence there are at most ℓk queues needed for such edges as H has queue number at most k.

This yields at most $\lfloor \frac{3}{2}\ell \rfloor$ intra-bag edges and at most $3\ell k$ inter-bag edges. ◂

Given a H-partition with bounded bichromatic layered-width, Claim 9 can obviously be refined as follows:

▸ **Lemma 10.** *For all graphs H and G, if H has a k-queue layout and G has a H-partition of bichromatic layered-width ℓ with respect to some bichromatic layering $(V_0, V_1, \dots)$ of G, then G has a $(2\ell k + \ell)$-queue layout using vertex order $\overrightarrow{V_0}, \overrightarrow{V_1}, \dots$, where $\overrightarrow{V_i}$ is some order of V_i. In particular,*

$$\mathrm{qn}(G) \leqslant 2\ell \ \mathrm{qn}(H) + \ell. \tag{2}$$

---

[1] Let (u, v) be an inter-layer inter-bag edge so that $u \in A_x$ and $v \in A_y$. Then, (u, v) is called *forward* if and only if x precedes y in the k-queue layout of H. Otherwise, it is called *backward*.

Proof. Since the layering is bichromatic, we observe that G contains no intra-layer edges. These are accounted with at most $\lfloor \frac{\ell}{2} \rfloor$ intra-bag queues (E.1) and at most $k\ell$ inter-bag queues (E.3) in the proof of Claim 9. Hence, the statement follows. ◂

Lemma 8 and Lemma 10 already imply that every planar bipartite graph G has a 33-queue layout (as planar 3-trees have queue number at most 5). This bound can be reduced to 28 following the modifications of Bekos et al. [7]. Namely, Bekos et al. apply the following modifications:

B.1 Additional constraints are maintained for a proper layered drawing algorithm for outer-planar graphs.

B.2 Based on (B.1), additional constraints for the 5-queue layout of planar 3-trees are shown.

B.3 *Degenerate tripods*[2] in the H-decomposition of G are excluded by inserting a three new vertices inside each face f of the triangulated graph G and triangulating appropriately. In particular, the three new vertices inside f become leafs in the augmented BFS-tree, that is, the BFS-layering of the original graph G stays intact.

B.4 Based on (B.1) to (B.3), the order of vertices within each layer is chosen more carefully when applying Claim 9.

As a result, Bekos et al. obtain the following:

▷ Claim 11 (Lemmas 5 and 6 of [7]). In the queue layout computed by the modifications (B.1) to (B.4) of the algorithm of Dujmović et al. [21], the intra-bag inter-layer edges (see E.2) can be assigned to at most 2 queues while each set of inter-bag edges (see (E.3) to (E.5)) can be assigned to at most 13 queues.

We are now ready to prove Theorem 1:

Proof of Theorem 1. By Lemma 8, for every bipartite planar graph G there is a H-partition with bichromatic layered width 3 such that H is planar and has treewidth at most 3. We then apply Lemma 10 and Claim 11. In particular, we observe that Claim 11 is applicable since none of the modifications described in Steps (B.1) to (B.4) interfere with our bichromatic layering. Namely, (B.1) and (B.2) directly operate on H while (B.3) and (B.4) respect the layering. Hence, by Claim 11, for bipartite planar graphs we need 2 queues for intra-bag inter-layer edges (E.2) and in total 26 queues for inter-bag inter-layer edges (E.4 and E.5) resulting in 28 queues overall. ◂

3 Structure of Stacked Quadrangulations

In this section we investigate the structure of stacked quadrangulations and then deduce an upper bound on the queue number. In particular we show that every stacked quadrangulation is a subgraph of the strong product $H \boxtimes C_4$, where H is a planar 3-tree. Recall that stacked quadrangulations are $(4,4)$-matching-stacked graphs. For ease of presentation, we first prove a product structure theorem for general (t,s)-stacked graphs as it prepares the proof for the matching variant.

▸ **Theorem 12.** *For $t \geqslant 3, s \geqslant 1$, every (t,s)-stacked graph G is a subgraph of $H \boxtimes K_s$ for some planar graph H of treewidth at most t.*

[2] A *tripod* is the content of a bag of H. It consists of a triangle from which three *vertical paths* (traversing the BFS-layering in order) emerge (and potentially some edges between such paths). In a *degenerate* tripod, one of the paths consists of a single vertex.

Proof. In order to prove the theorem, we need to find an H-partition of G, and a tree decomposition T of H with treewidth at most t, where H is a planar graph. Given a (t,s)-stacked graph G for $t \geqslant 3$ and $s \geqslant 1$ and its construction sequence, we define the H-partition $\big(H, \{V_x : x \in V(H)\}\big)$ of width at most s as follows. In the base case we have a graph of size at most s whose vertices all are assigned to a single bag V_{x_0}. Then in each construction step we add a new bag, say $V_{v'}$ that contains all new vertices (those of the inserted graph G'). Thus each bag contains at most s vertices, that is, the width of the H-partition is at most s. For $u \in V_x$ and $v \in V_y$, if G contains edge (u,v) then we connect x and y in H.

Next, we define a tree decomposition $\big(T, \{B_x : x \in V(T)\}\big)$ of H. We again give the definition iteratively following the construction sequence of G. We thereby maintain as an invariant that for each face f of the current subgraph of G, there is a bag B_{y_f} in T containing all vertices x of H for which V_x contains a vertex of f. In the base case, the tree decomposition contains a single bag that only contains node x_0. Now consider a recursive construction step, that is a connected graph G' of order at most s is inserted into some face f yielding a new (t,s)-stacked graph G''. Recall that there is a node v' in H with $V_{v'} = V(G')$. Let $F \subseteq V(H)$ denote the nodes x of H such that V_x contains a vertex of f. By induction hypothesis, there exists a node y_f in T such that B_{y_f} contains F. We add a new node y as a leaf of y_f associated with bag $B_y = F \cup \{v'\}$. We observe that this procedure indeed yields a tree decomposition of G''. Moreover, the new bag B_y contains all nodes of H that contain vertices of newly generated faces. Also note that each bag of T contains at most $t+1$ vertices, where t is the maximum size of a face in the construction process of G. Together with the observation that H is a minor of G and thus planar, this proves Theorem 12. ◂

We now extend our ideas to the following product structure theorem. Note that we use the same H-partition and show that the treewidth is at most $t-1$.

▸ **Theorem 13.** *For $t \geqslant 3, s \geqslant 2$, every (t,s)-matching-stacked graph G is a subgraph of $H \boxtimes K_s$ for some planar graph H of treewidth at most $t-1$.*

Proof. Given a (t,s)-matching-stacked graph G for $t \geqslant 3, s \geqslant 2$, we compute its H-partition and the tree decomposition T of H as in the proof of Theorem 12. By construction, the width of the H-partition is at most s and H is a minor of G and thus planar. So it suffices to show that each bag of T contains at most t nodes of H (instead of $t+1$). This is clearly true for the root-node of T whose bag has only one node of H. Consider a step in the construction of G, that is, we have a face f bounded by at most t vertices, and we place a connected subgraph G' of order at most s inside. Assume that each of the bags placed before introducing G' contains at most t nodes of H. Again, v' denotes the vertex of H with $V_{v'} = V(G')$, F is the set of nodes whose bags contain at least one vertex of f, and node y_f is the node whose bag B_{y_f} contains F. Further y is the node of H with $B_y = F \cup \{v'\}$ that is introduced as a leaf of y_f during this step.

We claim that F has at most $t-1$ nodes of H and therefore B_y contains at most t nodes. Consider the step where face f was created. During that step a subgraph G'' was added inside some face f'. So, if f is an interior face of G'', it follows that F contains only one node of H, namely v'' for which $V_{v''} = V(G'')$. On the other hand, as G'' is connected to the boundary of f' with a matching, at least two vertices of f belong to $V(G'')$. Hence the remaining vertices of f belong to at most $t-2$ bags associated with nodes of H and thus the set F has at most $t-1$ nodes as claimed. We conclude that each bag of the tree decomposition contains at most t nodes of H. ◂

Theorem 12 shows that every stacked quadrangulation is a subgraph of $H \boxtimes K_4$, where H is a planar graph with treewidth at most 4. However, stacked quadrangulations are also $(4,4)$-matching-stacked graphs and, hence, by Theorem 13 they are subgraphs of $H \boxtimes K_4$, where H is a planar 3-tree. In the following we improve this result by replacing K_4 by C_4.

▸ **Theorem 2.** *Every stacked quadrangulation is a subgraph of $H \boxtimes C_4$, where H is a planar 3-tree.*

Proof. Given a stacked quadrangulation G and its construction sequence, we compute its H-partition as described above. Note that in Theorem 13, we show that H is a planar 3-tree. It remains to show that H does not only certify that $G \subseteq H \boxtimes K_4$ (Theorem 13) but also the stronger statement that $G \subseteq H \boxtimes C_4$. That is, we need to show that in order to find G in the product, we only need edges that show up in the product with C_4. In each step of the construction of G we insert a 4-cycle into some face f. Hence, for each node x of H the bag V_x consists of a 4-cycle denoted by $(v_0^x, v_1^x, v_2^x, v_3^x)$. We label the four vertices with $0, 1, 2, 3$ such that for $i = 0, 1, 2, 3$ vertex v_{i+k}^x is labeled i for some offset k (all indices and labels taken modulo 4).

As the labels appear consecutively along the 4-cycle, the strong product allows for edges between two vertices of distinct bags if and only if their labels differ by at most 1 (mod 4). That is we aim to label the vertices of each inserted 4-cycle so that each inter-bag edge connects two vertices whose labels differ by at most 1. We even prove a slightly stronger statement, namely that offset k can be chosen for a newly inserted bag V_x such that the labels of any two vertices v and v' in G connected by an inter-bag edge differ by exactly 1. Indeed, assuming this for now, we see that if (v, v') is an inter-bag edge with $v \in V_x$ and $v' \in V_y$, then $(x, y) \in E(H)$. For this recall that V_x and V_y induce two 4-cycles. Assume that $v = v_i^x$ with label i and $v' = v_j^y$ is labeled j, where $0 \leqslant i, j \leqslant 3$. As the two labels differ by exactly 1, we have $j = i + 1 \pmod 4$ or $j = i - 1 \pmod 4$. Now in the strong product $H \boxtimes C_4$, vertex v_i^x is connected to all of $v_{i-1}^y, v_i^y, v_{i+1}^y$, that is, the edge (v, v') exists in $H \boxtimes C_4$. It is left to prove that the labels can indeed by chosen as claimed. As shown in Figure 1, starting with a 4-cycle with labels $0, 1, 2, 3$ from the initial 4-cycle, we obtain three types of faces that differ in the labeling of their vertices along their boundary: Type **(a)** has labels $i, i+1, i+2, i+3$, $(0 \leqslant i \leqslant 3)$, Type **(b)** has labels $i, i+1, i+2, i+1$, $(0 \leqslant i \leqslant 3)$, and Type **(c)** has labels $i, i+1, i, i+1$ $(0 \leqslant i \leqslant 3)$. In each of the three cases we are able to label the new 4-cycle so that the labels of the endpoints of each inter-bag edge differ by exactly 1, see Figure 1 and also Figure 2 for an example. This concludes the proof. ◂

Theorem 2 gives an upper bound of 21 on the queue number of stacked quadrangulations, compared to the upper bound of 5 on the queue number of planar 3-trees (stacked triangulations) [2].

▸ **Theorem 3.** *The queue number of stacked quadrangulations is at most* 21.

Proof. In general, we have that $\mathrm{qn}(H_1 \boxtimes H_2) \leqslant |V(H_2)| \cdot \mathrm{qn}(H_1) + \mathrm{qn}(H_2)$ by taking a queue layout of H_2 and replacing each vertex with a queue layout of H_1 [21, Lemma 9]. In particular, we conclude that $\mathrm{qn}(H \boxtimes C_4) \leqslant 4 \cdot \mathrm{qn}(H) + 1$. As the queue number of planar 3-trees is at most 5 [2], Theorem 2 gives an upper bound of $4 \cdot 5 + 1 = 21$. ◂

4 Lower Bounds

This section is devoted to lower bounds on the queue number and mixed page number of bipartite planar graphs. We use the same family of 2-degenerate quadrangulations $G_d(w)$ for

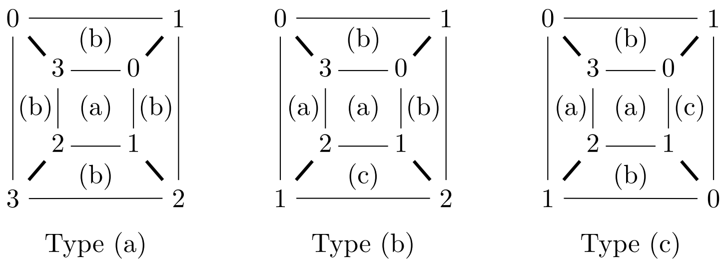

Figure 1 The three types of faces defined in the proof of Theorem 2, each with a 4-cycle stacked inside, where the labels represent the position of the vertex in the 4-cycle. For better readability, vertices are represented by their labels, where a vertex with label $i + j$ (same $i \in \{0, 1, 2, 3\}$ for all eight vertices) is written as j (labels taken mod 4). That is, each type represents four situations that can occur in a face, e.g., the other three cases of Type (b) have labels 1, 2, 3, 2 ($i = 1$), resp. 2, 3, 0, 3 ($i = 2$), resp. 3, 0, 1, 0 ($i = 3$) for the outer vertices and also plus i for the labels of the stacked 4-cycle. The inter-bag edges are drawn thick, and indeed the labels of their endpoints differ exactly by 1 (mod 4).

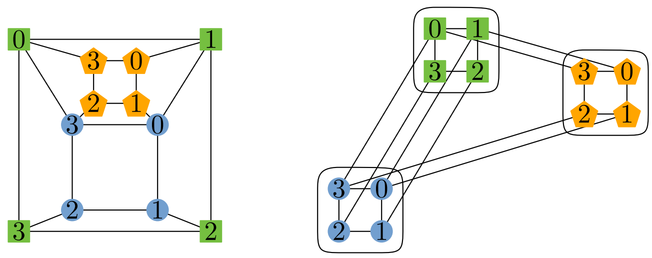

Figure 2 A stacked quadrangulation G with its H-partition showing $G \subseteq H \boxtimes C_4$, where H is a triangle in this case. The labels used in the proof of Theorem 2 are written inside the vertices.

both lower bounds. The graph $G_d(w)$ is defined as follows, where we call d the *depth* and w the *width* of $G_d(w)$; see Figure 3. Let $G_0(w)$ consist of two vertices, which we call *depth-0 vertices*. For $i \geqslant 0$, the graph $G_{i+1}(w)$ is obtained from $G_i(w)$ by adding w vertices into each inner face (except $i = 0$, where we use the unique face) and connecting each of them to the two depth-i vertices of this face (if two exist). If the face has only one depth-i vertex v on the boundary, then we connect the new vertices to v and the vertex opposite of v with respect to the face, that is the vertex that is not adjacent to v. The new vertices are then called *depth-*$(i + 1)$ *vertices*. Observe that the resulting graph is indeed a quadrangulation and each inner face is incident to at least one and at most two depth-$(i + 1)$ vertices. The two neighbors that a depth-$(i + 1)$ vertex u has when it is added are called its *parents*, and u is called a *child* of its parents. If two vertices u and v have the same two parents, they are called *siblings*. We call two vertices of the same depth a *pair* if they have a common child.

4.1 Queue Layouts

We prove combinatorially that $G_d(w)$ does not admit a 2-queue layout for $d \geqslant 3, w \geqslant 24$. We also verified with a SAT-solver [30] that the smallest graph in the family of queue number 3 is $G_4(4)$ containing 259 vertices.

▸ **Theorem 4.** *There is a 2-degenerate bipartite planar graph with queue number at least* 3.

Proof. We show that the queue number of $G_d(w)$ is at least 3 for $d \geqslant 4$ and $w \geqslant 24$. Assume

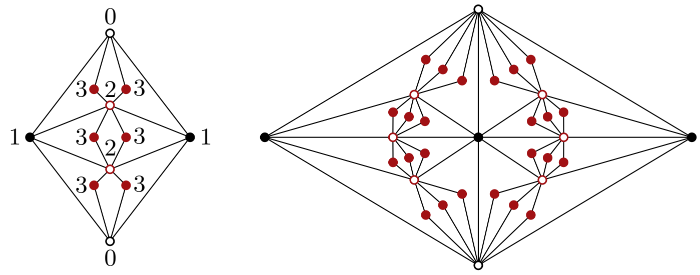

Figure 3 The graphs $G_3(2)$ and $G_3(3)$, where the numbers and style of the vertices indicate their depth.

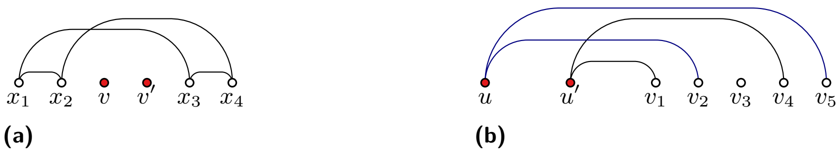

Figure 4 (a) A bad configuration with pair $\langle v, v' \rangle$. (b) A nested configuration with pair $\langle u, u' \rangle$.

to the contrary that $G_d(w)$ admits a 2-queue layout with vertex order $\prec$. Our goal is to determine some forbidden configurations that will lead to a contradiction. A *bad configuration* in a 2-queue layout of $G_d(w)$ consists of six vertices ordered $x_1 \prec x_2 \prec v \prec v' \prec x_3 \prec x_4$, where v and v' form a pair and (x_1, x_3, x_4, x_2) is a 4-cycle; see Figure 4a. A *nested configuration* consists of seven vertices $u \prec u' \prec v_1 \prec v_2 \prec v_3 \prec v_4 \prec v_5$, where u and u' form a pair, and contains edges (u, v_2), (u, v_4), (u', v_1) and (u', v_4); see Figure 4b. The *depth* of a configuration is defined as the depth of the pair $\langle v, v' \rangle$, respectively $\langle u, u' \rangle$.

▷ Claim 14. For $w \geqslant 14$, a 2-queue layout of $G_d(w)$ does not contain a bad configuration at depth $d' \leqslant d - 2$.

Proof. Consider a bad configuration and 14 children of v and v', partitioned into seven pairs. By pigeonhole principle, we have at least ten children between v and v' or we have at least three children either to the left of v or to the right of v'.

Assume first that we have at least three children of $\langle v, v' \rangle$ to the right of v' (note that the case where at least three children are to the left of v is symmetric). Clearly, we have two

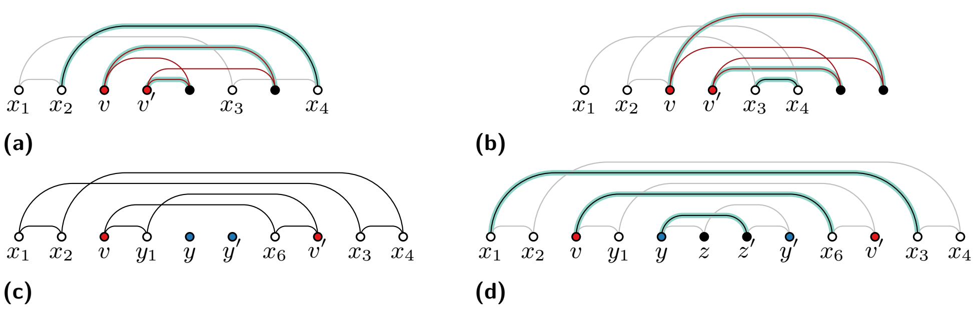

Figure 5 Proof of Claim 14. (a)–(b) A bad configuration with three children to the right of v'. Either two of them are to the left of x_4 as in (a) or to the right of x_4 as in (b). Both cases create a 3-rainbow. (c) If at least 10 children are between v and v', there is another bad configuration formed by v, v' and their children. (d) Three nested bad configurations contain a 3-rainbow.

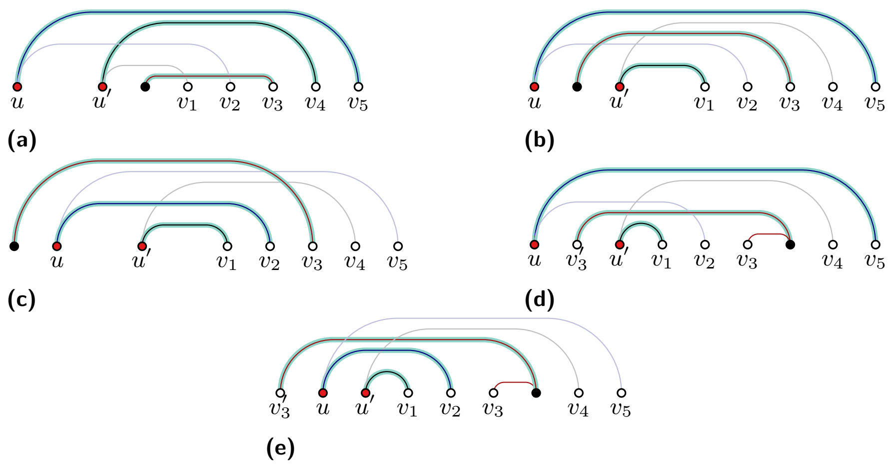

Figure 6 Proof of Claim 15. (a)–(c) Any edge leaving v_3 to the left creates a 3-rainbow. (d)–(e) The pair of v_3 does not precede u'.

children between v' and x_4 or two of them to the right of x_4 (see Figure 5). In both cases, the edges connecting them to v and v' form a 2-rainbow that is nested by (x_2, x_4) or nests (x_3, x_4), as shown in Figures 5a and 5b respectively. So we have that a 3-rainbow cannot be avoided if there are three children of v and v' to the right of v' or, by symmetry, to the left of v.

Second, assume that at least ten children of $\langle v, v'\rangle$ are placed between v and v', while at most four of them are not. We aim to find another bad configuration consisting of v, v', and four of their children. Since we have a total of 14 children forming seven pairs, and at most four children are not between v and v', it follows that at least three pairs of children are placed between v and v'. Let y_1 be the first child to the right of v and y_6 the first child to the left of v'. Then, at least one pair of children, say $\langle y, y'\rangle$, where $\{y_1, y_6\} \cap \{y, y'\} = \varnothing$ is placed between y_1 and y_6. Note that vertices v, y_1, y, y', y_6, v' form a new bad configuration at depth $d' + 1$, whose edges are nested by the edges of the starting bad configuration; the situation is depicted in Figure 5c.

We repeat the process and consider the children of $\langle y, y'\rangle$. If at least three of them are either to the left of y or the right of y', then there exists a 3-rainbow. Otherwise, there exists a pair of children $\langle z, z'\rangle$ of y and y' (at depth $d' + 2$) that are between y and y'. It is not hard to see that edges (x_1, x_3), (v, x_6) and (y, z') create a 3-rainbow; see Figure 5d. ◁

▷ Claim 15. If a 2-queue layout of $G_d(w)$ contains a nested configuration at depth $d' \leqslant d-1$, then v_3 precedes all its children. Additionally, if v_3 forms a pair with v_3', then v_3' is to the right of u'.

Proof. Consider a nested configuration at depth $d' < d$. Then v_3 has w children. If one of them is to the left of v_3, then it is either between u' and v_3, or between u and u' or to the left of u. In all three cases there is a 3-rainbow; see Figures 6a–6c. For the second part of the lemma, assume that v_3' precedes u'. Then it is either between u and u' or before u. Again a 3-rainbow is created; see Figures 6d and 6e. ◁

Consider the initial pair $\langle u, u'\rangle$ of $G_0(w)$ with 24 children, grouped into twelve pairs. Without loss of generality assume that $u < u'$ in a 2-layout of $G_d(w)$. If there are at least three pairs between u and u', then they form a bad configuration with u and u' at depth 0,

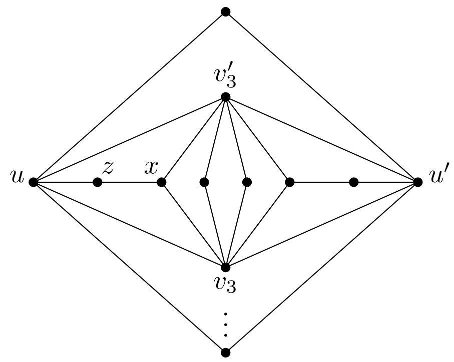

Figure 7 Parts of the graph whose queue number is at least 3 constructed for Theorem 4

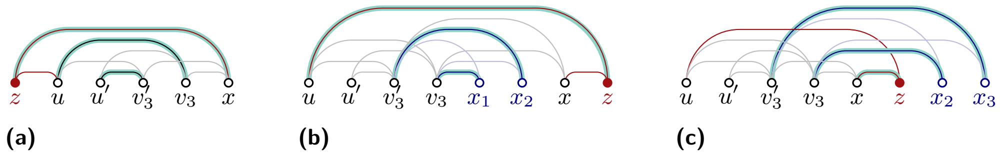

Figure 8 Three cases that can occur when inserting z into the layout without creating a bad configuration. In all three cases we have a 3-rainbow.

contradicting Claim 14. So, there are at most two pairs between u and u', and at least ten pairs have (at least) one vertex either to the left of u or the right of u'. Hence we can assume without loss of generality that at least five vertices of five different pairs are to the right of u'. Let v_1, v_2, v_3, v_4 and v_5 be these five vertices in the order they appear after u'. We assume without loss of generality that v_1, v_2, v_3, v_4 and v_5 are the rightmost possible choices, in particular, this means that for the pair $\langle v_i, v_i' \rangle$ it holds that $v_i' \prec v_i$, for $1 \leqslant i \leqslant 5$. As they are children of $\langle u, u' \rangle$, they form a nested configuration. By Claim 15 and the fact that $v_3' \prec v_3$, we conclude that v_3' is between u' and v_3, while the children of $\langle v_3, v_3' \rangle$ are to the right of v_3.

Now consider the children of $\langle v_3, v_3' \rangle$ and let x denote the child that shares a face with u. Denote by x_i, $1 \leqslant i \leqslant 3$, any three children different from x such that $x_1 \prec x_2 \prec x_3$; see Figure 7. By Claim 15, all children of $\langle v_3, v_3' \rangle$ are to the right of v_3. In particular, either $x_1 \prec x_2 \prec x$ or $x \prec x_2 \prec x_3$. As u and x belong to the boundary of a face, and x is at depth $2 < d$, u and x have w common children. By Claim 14, there exists a pair of children $\langle z, z' \rangle$ of $\langle u, x \rangle$ such that z is not located between u and x. Hence there are two cases to consider, namely z is to the left of u, or z is to the right of x. In the first case, edges (u', v_3'), (u, v_3) and (x, z) form a 3-rainbow; see Figure 8a. So, z is to the right of x. If $x_1 \prec x_2 \prec x$, then we have the situation depicted in Figure 8b, otherwise $x \prec x_2 \prec x_3$ as in Figure 8c. In both cases a 3-rainbow is created. We conclude that $G_d(w)$ with $d = 4$ and $w = 24$ does not admit a 2-queue layout. ◂

4.2 Mixed Linear Layouts

Next, we prove that for $d \geqslant 3$ and $w \geqslant 154$, graph $G_d(w)$ does not admit a 1-queue 1-stack layout. We remark that the smallest graph of this family with this property is actually $G_3(5)$ which has 128 vertices. Again, we verified this with a SAT-solver [30]. Note that the following theorem answers a question raised in [3, 18, 31].

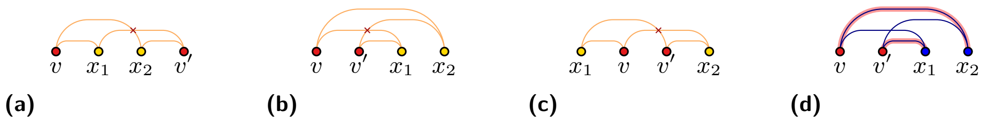

Figure 9 Children of a pair $\langle v, v'\rangle$ with $v \prec v'$. (a) There is at most one orange child between v and v'. (b)–(c) There is at most one orange child to the left of v or to the right of v'. (d) There is at most one blue child to the right of v'.

▸ **Theorem 5.** *There is a 2-degenerate bipartite planar graph that does not admit a 1-queue 1-stack layout.*

Proof. Assume for the sake of a contradiction that $G_3(154)$ admits a 1-queue 1-stack layout with vertex order $\prec$ and let u, u' denote the two initial vertices with $u \prec u'$. For ease of presentation, we call an edge *blue* (*orange*) if it is in the queue (stack) and color the edges accordingly in all figures. We distinguish three types of children: A child x with parent pair $\langle v, v'\rangle$ is called a *blue (orange) child* if both edges (v, x) and (v', x) are blue (orange, resp.), and it is called *bicolored* if one of the edges is blue and the other is orange. A pair is called *blue* (*orange*) if both vertices are blue (orange) and *bicolored* if it contains a bicolored vertex.

Consider a pair $\langle v, v'\rangle$ with $v \prec v'$. We first make two preliminary observations.

▷ Claim 16. A pair $\langle v, v'\rangle$ with $v \prec v'$ has at most two orange children, one between v and v' and one to the left of v or to the right of v'.

Proof. Suppose first that $\langle v, v'\rangle$ has two orange children x_1, x_2 such that $v \prec x_1 \prec x_2 \prec v'$. Then, edges (v, x_2) and (v', x_1) cross (Figure 9a), a contradiction. Second, consider the case $v \prec v' \prec x_1 \prec x_2$ (the case $x_1 \prec x_2 \prec v \prec v'$ is symmetric). Here (v, x_1) and (v', x_2) cross (Figure 9b). Finally, if $x_1 \prec v \prec v' \prec x_2$, then (x_1, v') and (x_2, v) cross (Figure 9c). ◂

▷ Claim 17. A pair $\langle v, v'\rangle$ has at most two blue children that are not located between v and v', namely one to the left of v and one to the right of v'.

Proof. Assume for a contradiction that $\langle v, v'\rangle$ has two blue children x_1, x_2 to the right of v'. Then, edges (v, x_2) and (v', x_1) nest (Figure 9d); a contradiction. ◃

We group the children of every pair $\langle v, v'\rangle$ at depth $d' < d$ into 77 pairs each. Then, we ignore any pair containing a blue vertex that is not placed between its parents or containing a orange vertex (no matter where it is placed). That is, by Claims 16 and 17 we discard at most four pairs of children for each pair $\langle v, v'\rangle$, that is at least 146 children out of 154 that are grouped into 73 pairs remain. Let G' denote the resulting subgraph of $G_d(w)$. By definition of subgraph G', the following property holds:

▷ Claim 18. Let $\langle v, v'\rangle$ denote a pair occurring in G'. Then (i) $\langle v, v'\rangle$ is either bicolored or blue in G' and (ii) all blue children of $\langle v, v'\rangle$ in G' are placed between v and v' in $\prec$.

We now consider the 146 children of a pair $\langle u, u'\rangle$ at depth $d' \leqslant d-2$ in the linear layout of G' induced by the linear layout of G, grouped into 73 pairs. Consider the following configuration. The pair $\langle u, u'\rangle$ has five pairs $\langle v_i, v_i'\rangle$ (for $1 \leqslant i \leqslant 5$) of children and pair $\langle v_i, v_i'\rangle$ has a child z_i. We call this is a *mixed configuration* if (i) $u, u', v_i' \prec v_i$, (ii) (u, v_i) is orange while (u', v_i) is blue, (iii) all edges (v_i, z_i) (for $1 \leqslant i \leqslant 5$) have the same color; see Figure 10.

▷ Claim 19. In the mixed layout of G', there is no mixed configuration with edges (v_i, z_i) (for $1 \leqslant i \leqslant 5$) being blue.

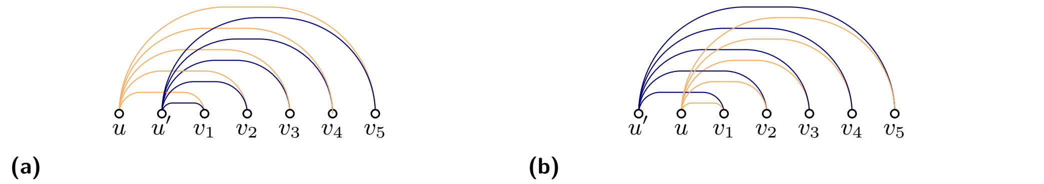

Figure 10 The two different possible layouts of vertices $u, u', v_1, \ldots, v_5$ of a mixed configuration.

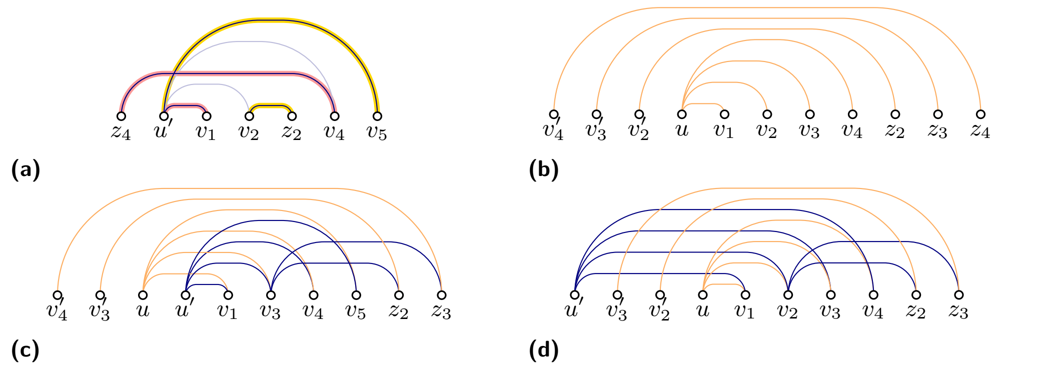

Figure 11 The edges v_iz_i are blue. Connecting v_3' to its parents u and u' yields a contradiction.

Proof. Observe that, for $2 \leqslant i \leqslant 4$, $v_5 \prec z_i$ as otherwise (v_i, z_i) nests (u', v_1) or is nested by (u', v_5); see Figure 11a. Thus by Claim 18(ii), vertices z_2, z_3, z_4 are bicolored and therefore edges $(v_2'z_2)$, $(v_3'z_3)$ and (v_4', z_4) are orange. As orange edges may not cross, v_2', v_3', v_4' are to the left of u (we already have $v_i' \prec v_i$ by the definition of a mixed configuration). In particular $v_4' \prec v_3' \prec v_2' \prec u$; see Figure 11b. Note that we do not know the position of u' in the vertex order so far. First assume that $v_3' \prec u'$; see Figure 11c, where u is drawn to the left of u' as in Figure 10a (note that the following argument also applies if $u' \prec u$ as in Figure 10b). As $v_4' \prec v_3'$, vertex v_4' is to the left of both u and u' and therefore bicolored, by Claim 18(ii). However, the edges (v_4', u) and (v_4', u') both cross the orange edge (v_3', z_3). Thus, we have $u' \prec v_3'$; see Figure 11d. Here it holds that $u' \prec v_3' \prec v_2' \prec u \prec v_1$. In this case, edge (v_3', u) is nested by the blue edge (u', v_1), hence, it cannot be blue. On the other hand, it crosses the orange edge (v_2', z_2), so it cannot be orange either. ◁

▷ Claim 20. In the mixed layout of G', there is no mixed configuration with edges (v_i, z_i) (for $1 \leqslant i \leqslant 5$) being orange.

Proof. Consider edge (v_i, z_i) for $2 \leqslant i \leqslant 4$. If z_i is to the left of v_{i-1} then it crosses the orange edge (u, v_{i-1}), and if it is to the right of v_{i+1} then it crosses the orange edge (u, v_{i+1}); see Figure 12a. So $v_1 \prec z_2 \prec z_4 \prec v_5$ holds. Recall that G' contains no orange children so for $1 \leqslant i \leqslant 5$, the edge $(v_i'z_i)$ is blue. Since (u', v_1) is blue, for $2 \leqslant i \leqslant 5$, v_i' cannot precede u',

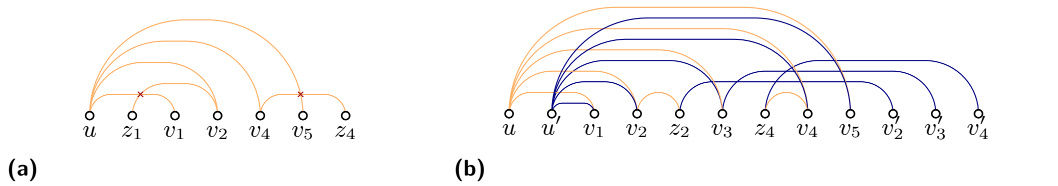

Figure 12 The edges y_ic_i are orange. Connecting v_4' to its parents u and u' yields a contradiction.

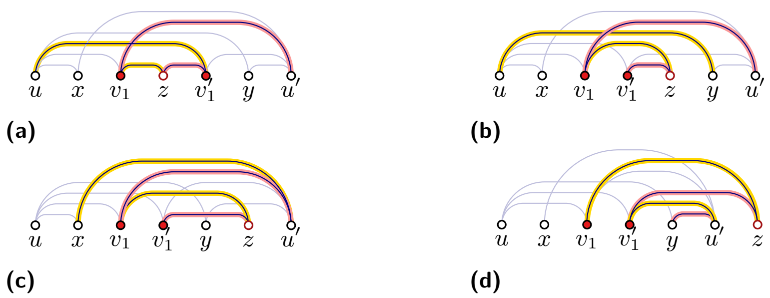

Figure 13 If there are three blue pairs between u and u', one of them, namely $\langle v_1, v_1' \rangle$, is between a vertex x and a vertex y belonging to other blue pairs. A child z of $\langle v_1, v_1' \rangle$ results in a nesting.

as otherwise (v_i', z_i) would nest (u', v_1). Similarly, since (u', v_5) is blue, for $1 \leqslant i \leqslant 4$, vertex v_i' cannot be between u' and v_5, as otherwise (v_i', z_i) would be nested by (u', v_5). Thus, we conclude that $v_5 \prec v_2' \prec v_3' \prec v_4'$; see Figure 12b. Since v_4' is to the right of u and u', by Claim 18, it must be bicolored, that is, either edge (u, v_4') or edge (u', v_4') is blue. However, both these edges nest the blue edge (v_2', z_2), a contradiction. ◁

Combining Claims 19 and 20, we conclude that the linear layout of G' contains no mixed configuration. This property allows us to conclude the following:

▷ Claim 21. Let $\langle u, u' \rangle$ be a pair in G' at depth $d' \leqslant d - 2$. In the linear layout of G' there exist at least five pairs of children of $\langle u, u' \rangle$ with both vertices of each pair between u and u'.

Proof. Assume for the sake of contradiction that $\langle u, u' \rangle$ have at most four such pairs of children. Thus, for at least 69 pairs, at least one vertex is not located between u and u'. In particular, at least 35 of these vertices either precede both u and u', or are placed to the right of both u and u'. Assume without loss of generality that the latter applies. Recall that children to the right of both parents are bicolored by Claim 18(ii). Now, among these 35 bicolored children, at least 18 are connected to the same parent u or u' with an orange edge; without loss of generality to u. These 18 children belong to at least 9 pairs, so we can select nine of them that do not form a pair, and in particular we select the nine rightmost ones, say v_1 to v_9. Observe that $v_i' \prec v_i$, for $1 \leqslant i \leqslant 9$. Indeed, if v_i' is bicolored and $v_i \prec v_i'$, then v_i' would have been chosen instead of v_i. On the other hand, if v_i' is blue, then it is located between u and u' by Claim 18(ii) and thus $v_i' \prec v_i$. Now let z_i be a child of $\langle v_i, v_i' \rangle$ $(1 \leqslant i \leqslant 9)$. By the pigeonhole principle, either five of the edges (v_i, z_i) with $1 \leqslant i \leqslant 9$ are blue or five of these edges are orange. Hence a mixed configuration is formed, contradicting Claims 19 and 20. ◁

Since $d > 2$, we conclude that there are pairs $\langle u, u' \rangle$ which have at least five pairs of children for which both vertices are located between u and u'. We now investigate this case.

▷ Claim 22. Let $\langle u, u' \rangle$ be a pair at depth $d' \leqslant d - 2$. In the linear layout of G' there is a pair $\langle v, v' \rangle$ of children of $\langle u, u' \rangle$, so that no child of $\langle v, v' \rangle$ is located between v and v'.

Proof. By Claim 21, the pair $\langle u, u' \rangle$ has five pairs of children $\langle v_1, v_1' \rangle, \ldots, \langle v_5, v_5' \rangle$ for which both vertices are located between u and u'. Assume without loss of generality that $u \prec u'$. As there are no orange pairs in G', either three of them are blue or three of them are bicolored. Assume first that three of these pairs, say $\langle v_1, v_1' \rangle$, $\langle v_2, v_2' \rangle$, $\langle v_3, v_3' \rangle$ are blue. Then there is a blue pair among them, say without loss of generality $\langle v_1, v_1' \rangle$, such that $u \prec x \prec v_1 \prec v_1' \prec y \prec u'$ where $x, y \in \{v_2, v_2', v_3, v_3'\}$. Now consider any child z of v_1 and v_1'.

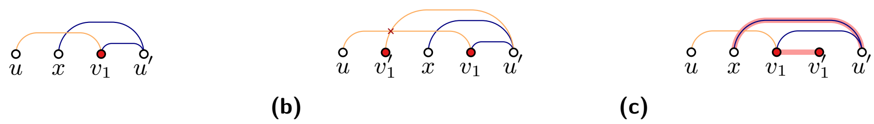

Figure 14 Three bicolored pairs $\langle v_i, v_i' \rangle$ of children of $\langle u, u' \rangle$ are between u and u'. (a) Without loss of generality vertex v_1 is nested by a blue edge. (b) Vertex v_1' does not precede x. (c) Blue and bicolored children of $\langle v_1, v_1' \rangle$ are to the left or to the right of both parents.

Since by definition G' contains no orange children, z is connected with a blue edge to either v_1 or v_1'. Vertex z may be placed either to the left of v_1, or between v_1 and v_1' or to the right of v_1'. If it is between v_1 and v_1', the edge (v_1, z) is nested by (u, v_1') and the edge (z, v_1') is nested by (v_1, u'); see Figure 13a. Thus z cannot be connected to v_1 or v_1' with a blue edge; a contradiction. Assume without loss of generality that z is to the right of v_1'. It is easy to verify that for all possible placements of z, the blue edge connecting z to v_1 or v_1' either nests or is nested by an edge incident to one of u and u'; see Figures 13b–13d.

Thus, there are three bicolored pairs between u and u', say $\langle v_1, v_1' \rangle$, $\langle v_2, v_2' \rangle$, $\langle v_3, v_3' \rangle$, such that v is a bicolored vertex while v' can be blue or bicolored. Without loss of generality two of v_1, v_2, v_3, say v_1 and v_2 are connected to u with an orange edge. Let x be the leftmost among $v_1, v_1', v_2, v_2', v_3, v_3'$ in $\prec$ that is connected to u' with a blue edge. As a result for one of v_1 and v_2, say without loss of generality v_1, we have $v_1' \neq x$ and $u \prec x \prec v_1 \prec u'$; see Figure 14a. Observe that $x \prec v_1'$. Otherwise (v_1', u') cannot be blue by the choice of x and cannot be orange either, as it would cross the orange edge (u, v_1); see Figure 14b. Now the blue edge (x, u') nests above v_1 and v_1' and thus blue and bicolored children of $\langle v_1, v_1' \rangle$ cannot be between them; see Figure 14c. ◁

We are now ready to prove the theorem. Namely, we have the initial pair $\langle u, u' \rangle$ of $G_0(w)$ at depth $0 \leqslant d-2$. Then, by Claim 21 there is a pair $\langle v, v' \rangle$ at depth 1 such that no child of $\langle v, v' \rangle$ is located between v and v'. Since however $\langle v, v' \rangle$ is at depth $1 \leqslant d-2$, by Claim 21, at least 10 of the children of $\langle v, v' \rangle$ must be between v and v' in $\prec$; a contradiction. ◂

In contrast to our result on the queue number of bipartite planar graphs (Theorem 4), bipartite planar graphs admit 2-stack layouts. Therefore, if we increase the number of stacks, we can easily construct a mixed linear layout of $G_d(w)$ (or of any bipartite planar graph). On the other hand, it remains open how many queues are needed if we allow at most one stack. In the next section we approach this question by showing that the graph $G_d(w)$ constructed above (and even more generally any 2-degenerate quadrangulation) admits a 5-queue layout.

5 2-Degenerate Quadrangulations

Note that the graph $G_d(w)$ defined in Section 4 is a 2-degenerate quadrangulation. Recall that it can be constructed from a 4-cycle by repeatedly adding a degree-2 vertex and keeping all faces of length 4. Hence, every 2-degenerate quadrangulation is a subgraph of a 4-tree. This can also be observed by seeing $G_d(w)$ as a $(4,1)$-stack graph, together with Theorem 12. Thus, by the result of Wiechert [34], it admits a layout on $2^4 - 1 = 15$ queues. In this section, we improve this bound by showing that 2-degenerate quadrangulations admit 5-queue layouts.

Our proof is constructive and uses a special type of tree-partition. Let T be a tree-partition of a given graph G, that is, an H-partition where H is a rooted tree. For every node x of T, if y is the parent node of x in T, the set of vertices in T_y having a neighbor in T_x

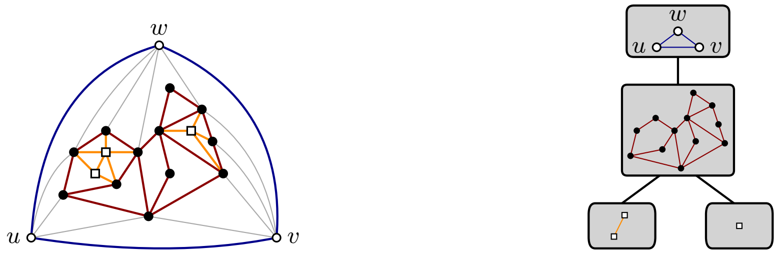

Figure 15 A planar graph and its tree-partition of shadow width 4.

is called the *shadow* of x; we say that the shadow is *contained* in node y. The *shadow width* of a tree-partition is the maximum size of a shadow contained in a node of T; see Figure 15.

Let $\mathcal{S} = \{C_i \subseteq V \,:\, 1 \leqslant i \leqslant |\mathcal{S}|\}$ be a collection of vertex subsets for a graph $G = (V, E)$, and let π be an order of V. Consider two elements from $\mathcal{S}$, $C_x = [x_1, x_2, \dots, x_{|C_x|}]$ and $C_y = [y_1, y_2, \dots, y_{|C_y|}]$, where the vertices are ordered according to π. We say that C_x *precedes* C_y with respect to π if $x_i \leqslant y_i$, for all $1 \leqslant i \leqslant \min(|C_x|, |C_y|)$; we denote this relation by $C_1 \prec C_2$. We say that $\mathcal{S}$ is *nicely ordered* if $\prec$ is a total order on $\mathcal{S}$, that is, $C_i \prec C_j$ for all $1 \leqslant i < j \leqslant |S|$. A similar concept of clique orders has been considered in [22] and [32].

Lemma 23. *Let $G = (V, E)$ be a graph with a tree-partition $\big(T, \{T_x : x \in V(T)\}\big)$ of shadow width k. Assume that for every node x of T, the following holds: (i) there exists a q-queue layout of T_x with vertex order π, and (ii) all the shadows contained in x are nicely ordered with respect to π. Then* $\mathrm{qn}(G) \leqslant q + k$.

Proof. In order to construct a desired queue layout of G, we first build a 1-queue layout of the nodes of T. This is done by lexicographic breadth-first search (starting from the root of T) in which the nodes sharing the same parent are ordered with respect to the given nice order of shadows. Then every node, x, in the layout is replaced by the vertices of bag T_x; the vertices within a bag are ordered with respect to the vertex order π of the q-queue layout that is guaranteed by the lemma. This results in an order of the vertices of G in which every vertex $v \in V$ is associated with a pair $\langle i_v, j_v \rangle$, where i_v is derived from the 1-queue layout of T and j_v is derived from π. Clearly, the vertices are ordered lexicographically with respect to their pairs.

Now we show how to obtain a $(q + k)$-queue layout using the resulting vertex order. To this end, we use q queues for the intra-bag edges and separate k queues for inter-bag edges. It is easy to see that the intra-bag edges do not nest (as the bags are separated in the order); therefore, we only need to verify that inter-bag edges fit in k queues.

Consider two edges, $e_1 = (u_1, v_1)$ and $e_2 = (u_2, v_2)$ of G. Since the layout is derived from a 1-queue layout of T, the edges may nest only when u_1 and u_2 are from the same bag; let x be the bag such that $u_1, u_2 \in T_x$. Assign inter-bag edges rooted at x to k queues respecting the nice order of the shadows. That is, edges incident to the first vertices of the shadows are in the first queue, edges incident to the second vertices of the shadows are in the second queue and so on. Since the shadow order is nice and every shadow is of size $\leqslant k$, there are at most k queues in the layout. ◂

Before applying Lemma 23 to 2-degenerate quadrangulations, we remark that the result provides a 5-queue layout of planar 3-trees, as shown by Alam et al. [2]. Indeed, a breadth-first search (starting from an arbitrary vertex) on 3-trees yields a tree-partition in which every bag is an outerplanar graph. The shadow width of the tree-partition is 3 (the length of each face), and it is easy to construct a nicely ordered 2-queue layout for every outerplanar graph [23]. Thus, Lemma 23 yields a 5-queue layout for planar 3-trees. Now we turn our attention to 2-degenerate quadrangulations.

▸ **Lemma 24.** *Every* 2*-degenerate quadrangulation admits a tree-partition of shadow width* 4 *such that every bag induces a leveled planar graph.*

Proof. Recall that 2-degenerate quadrangulations admit a recursive construction starting from a 4-cycle. At each step a vertex v of degree 2 is added inside a 4-face $f = (u_1, u_2, u_3, u_4)$ of the constructed subgraph, such that v is connected to two opposite vertices of f, that is v is connected either to u_1 and u_3 or to u_2 and u_4. This construction yields a total order $v_1 < v_2 < \cdots < v_n$ on the vertices of the input 2-generate quadrangulation G of order n, such that v_1, v_2, v_3, v_4 are the vertices of the starting 4-cycle, and $v_{i\geqslant 5}$ is the vertex added at step i. This order is not unique, as one may permute the starting four vertices, or (possibly) select a different vertex to add at each step. Assume that vertices u_1, u_2, $\ldots$ u_k $(k \geqslant 1)$ that are added at steps $i_1 < i_2 < ... < i_k$ (that is $u_s = v_{i_s}$), are connected to the same two vertices v_j and $v_{j'}$ of G, with $j < j' < i_1$. Following the definitions given in Section 4, we say that vertices u_1, u_2, $\ldots$ u_k are siblings with parents v_j and $v_{j'}$. Note that at step i_1, any vertex among u_1, u_2, $\ldots$ u_k may be added, and in particular they can all be added at consecutive steps.

Our goal is to assign a *layer value* $\lambda(v)$ to each vertex v of G such that (i) the subgraph G_λ induced by vertices of layer λ $(\lambda \geqslant 0)$ is a leveled planar graph, and (ii) the connected components of all subgraphs G_λ define the bags of a tree-partition of shadow width 4. Note that we will assign layer values that do not necessarily correspond to a BFS-layering of G.

The four vertices of the starting 4-cycle have layer value equal to 0. Consider now a set of siblings $u_1, \ldots, u_k$ with parents v and v', that are placed inside a 4-face $f = (v, w, v', w')$ of the constructed subgraph. We compute the layer value of vertices $u_1, \ldots, u_k$ as follows. Assume without loss of generality that $\lambda(v) \leqslant \lambda(v')$ and $\lambda(w) \leqslant \lambda(w')$. Further, assume that $u_1, \ldots, u_k$ are such that the cyclic order of edges incident to v are $(v, w), (v, u_1), (v, u_2), \ldots, (v, u_k), (v, w')$ whereas the cyclic order of edges incident to v' are $(v', w'), (v', u_k), (v', u_{k-1}), \ldots, (v', u_1), (v', w)$; see Figure 16. We will insert these vertices in the order $u_1, u_k, u_2 \ldots, u_{k-1}$, that is, u_1 is inserted inside $f_1 = f$, u_k inside $f_k = (v, u_1, v', w')$ and every subsequent u_i inside $f_i = (v, u_{i+1}, u_k, w')$. Then the layer value of vertex u_i is defined as $\lambda(u_i) = 1 + \min\{\lambda(x), x \in f_i\}$, for $1 \leqslant i \leqslant k$. In the following, we will associate f with the layer values of its vertices, that is we call f a *[*$\lambda(v)$,$\lambda(w)$,$\lambda(v')$,$\lambda(w')$*]-face*, where vertices v and v' form a pair whose children are placed inside f.

Note that, by the definition of the layer values, if a vertex u that is placed inside a face f has layer λ, then all vertices of f have layer value $\lambda - 1$ or λ. This implies that connected components of layer λ are adjacent to at most four vertices of layer value $\lambda - 1$ (that form a 4-cycle).

To simplify the presentation, we focus on a [0,0,0,0]-face f_0 and our goal is to determine the subgraph of layer value 1 placed inside it; an analogous approach is used for the interior of a [λ,λ,λ,λ]-face, with $\lambda > 0$.

[0,0,0,0]-face: In this case, all vertices $u_1, \ldots, u_k$ will have layer value 1 (see Figure 16a). The newly created faces (w, v, u_1, v') and (w', v, u_k, v') are [0,0,1,0]-faces, while all other faces u_i, v, u_{i+1}, v' for $i = 1, \ldots, k-1$ are $[1, 0, 1, 0]$-faces.

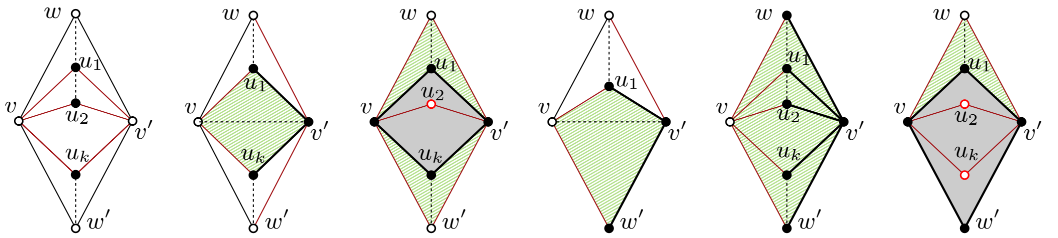

(a) $[0,0,0,0]$ **(b)** $[0,0,1,0]$ **(c)** $[1,0,1,0]$ **(d)** $[0,0,1,1]$ **(e)** [0,1,1,1] **(f)** [1,0,1,1]

Figure 16 Cases for faces that contain a set of children in their interior. Vertices at layer values 0, 1 and 2 are drawn as black circles, black disks and red circles resp. Edges that connect vertices of the same (different) layer value are drawn black (red resp.). The dotted diagonals inside a face connect the parents of the children placed inside. Faces of type [0,1,1,1] are shaded in green, and faces that contain vertices of layer value at least 2 are shaded in gray.

[0,0,1,0]-face: We continue with a $[0,0,1,0]$-face and then consider a $[1,0,1,0]$-face. In a $[0,0,1,0]$-face, we add only vertices u_1 and u_k, which creates the $[0,0,1,1]$-faces (w, v, u_1, v') and $(w,' v, u_k, v')$, and one [0,1,1,1]-face (v, u_1, v', u_k) (see Figure 16b). Note that the remaining siblings $u_2, \ldots, u_{k-1}$ will be added as children of v and v' inside face (v, u_1, v', u_k).

[1,0,1,0]-face: In a $[1,0,1,0]$-face, vertices u_1 and u_k have layer value 1, while all other siblings u_i, $i = 2, \ldots, k-1$ have layer value 2. Note that in a BFS-layering, vertex u_1 would have layer value 2 instead of 1. In this case, (w, v, u_1, v') and (w', v, u_k, v') are [0,1,1,1]-faces, while the other faces cannot contain vertices of layer value 1 (see Figure 16c). In total, we have two new types of faces, namely $[0,0,1,1]$ and [0,1,1,1]-faces.

[0,0,1,1]-face: In a $[0,0,1,1]$-face, we add only vertex u_1, which creates two faces, namely the $[0,0,1,1]$-face (w, v, u_1, v'), and the [0,1,1,1]-face (v, w', v', u_1). Note that the remaining vertices $u_2, \ldots, u_k$ will be added as children of v and v' inside face (v, w', v', u_1); see Figure 16d.

[0,1,1,1]-face: Finally, a [0,1,1,1]-face is split into $k+1$ faces of type [1,0,1,1] (see Figure 16f). In a [1,0,1,1]-face, only vertex u_1 has layer value 1, and face (w, v, u_1, v') is of type [0,1,1,1] (see Figure 16e).

In order to create a layered planar drawing, we first consider faces of type [0,1,1,1], since they are contained in almost all other types of faces. The existence of k children in such a face f creates $k+1$ faces of type [1,0,1,1]. Let g_i be the face (u_i, v, u_{i+1}, v') of type [1,0,1,1], for $i = 0, \ldots, k$, where $u_0 = w$ and $u_{k+1} = w'$. If another set of children $u'_1, \ldots, u'_{k'}$ is added inside g_i then their parents are vertices u_i and u_{i+1} and only u'_1 has layer value 1. Hence the addition of u'_1 creates a new [0,1,1,1]-face g'_i (namely face (v, u_i, u'_1, u_{i+1})). Further addition of children inside g'_i, will split g'_i into faces of type [1,0,1,1]. So, let G_f be the subgraph induced by all vertices of layer value 1 inside a [0,1,1,1]-face f (including its boundary vertices).

▷ Claim 25. The subgraph G_f of a [0,1,1,1]-face $f = (v, w, v', w')$ has a leveled planar drawing such that level 0 contains one vertex among w, v' and w' (and no other vertex); see Figures 17a-17c.

Proof. Based on the previous observation, we will create a sequence $\{G_f^i\}_{1 \leqslant i \leqslant s}$ such that G_f^i is a subgraph of G_f^{i+1} and G_f^s is G_f. Let H_f^i be the subgraph of G induced by the vertices of G_f^i and vertex v. In our construction, graphs G_f^i will have the following properties: (i)

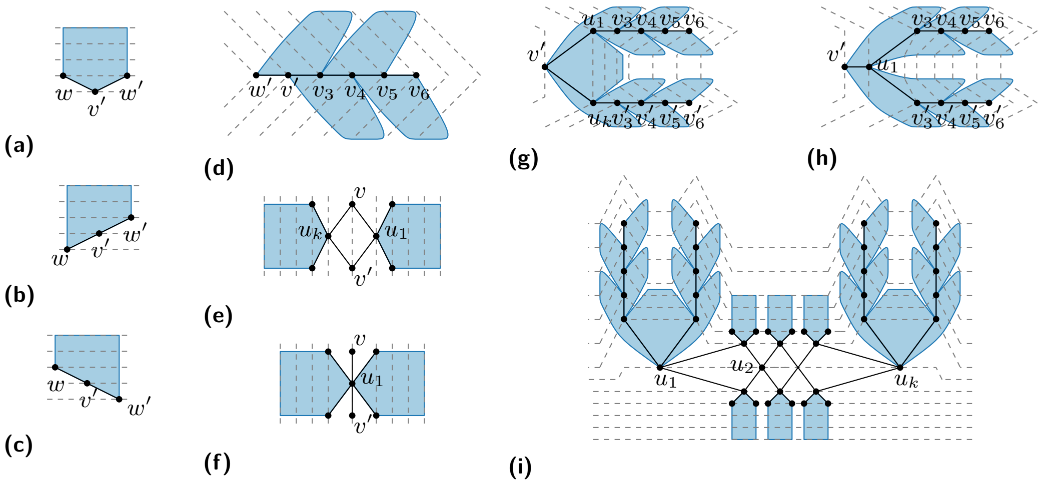

Figure 17 Illustrations of Γ_f when f is (a)–(c) a [0,1,1,1]-face, (d) a [0,0,1,1]-face, (e)–(f) a [1,0,1,0]-face, (g)–(h) a [0,0,1,0]-face, and (i) a [0,0,0,0]-face.

the interior faces of G_f^i are of type [1,1,1,1], (ii) H_f^i contains all [1,1,1,1]-faces of G_f^i and every other interior face is of type [1,0,1,1] with vertex v on its boundary.

At the first step G_f^1 consists of vertices v', w, w' and the $k_{v'}$ siblings of v and v'. The subgraph so far is a star with v' as center. It is not hard to see the G_f^1 satisfies Properties (i) and (ii). At step i we select a [1,0,1,1]-face f_i of H_f^{i-1} (that is not empty). Let $f_i = (v, u_i, v_i, u_i')$, and let w_i be the only child of layer value 1 inside f_i (with parents v and v_i). Then f_i is split into the [1,1,1,1]-face (v, w_i, v_i, u_i') and the [0,1,1,1]-face $f_i' = (v, u_i, w_i, u_i')$. Further let $x_1, \dots x_k$, $k \geqslant 0$, be the children inside f_i'. Recall that $x_1, \dots x_k$ have layer value 1 and their parents are v and w_i. We obtain G_f^i from G_f^{i-1} by adding a star with center w_i and vertices $x_1, \dots x_k$ as leafs, and by connecting w_i to vertices u_i and u_i' so that vertices $x_1, \dots x_k$ are on the outer face of G_f^i. As face f_i of H_f^{i-1} is split into a [1,1,1,1]-face and $k+1$ [1,0,1,1]-faces, it follows that G_f^i contains one more interior [1,1,1,1]-face than G_f^{i-1} (that is Property (i) is satisfied), and all other interior faces of H_f^i are of type [1,0,1,1] with v on their boundary (Property (ii)).

Now we show how to construct the leveled planar drawing of G_f based on the sequence $\{G_f^i\}_{1 \leqslant i \leqslant s}$. In particular, we will extend a leveled planar drawing Γ_f^{i-1} of G_f^{i-1} to a leveled planar drawing Γ_f^i of G_f^i, for $1 < i \leqslant s$. For every [1,0,1,1]-face f_j of H_f^{i-1} (for some $j \geqslant i$) with vertices v, u_j, v_j, u_j' we denote as P_j the path (u_j, v_j, u_j'), and say that P_j is the *boundary path* of f_j. Note that P_j is along the outer face of Γ_f^{i-1}. We say that P_j forms a *small angle* in Γ_f^{i-1} if $\ell(u_j) = \ell(u_j') = \ell(v_j) + 1$ holds, where $\ell(u)$ is the level of vertex u; see Figure 18a. We also say that P_j forms a *large angle* if either $\ell(v_j) = \ell(u_j) + 1 = \ell(u_j') - 1$ or $\ell(v_j) = \ell(u_j') + 1 = \ell(u_j) - 1$ holds; see Figures 18b and 18c. Our algorithm maintains the following invariants: (i) level 0 contains one of vertices w, v' or w' of f (and no other vertices), (ii) vertices v_i and $x_1, \dots, x_k$ of G_f^i are placed in the outer face of Γ_f^{i-1}, and (iii) every path P_j of G_f^i forms either a small or a large angle along the outer face of Γ_f^i .

Three different leveled planar drawings of G_f^1 are shown in Figure 19. We have that $f_1 = (v, u_1, w_1, u_1')$, where $u_1 = w$, $u_1' = w'$ and $w_1 = v'$ (refer to Figure 16f). It is not hard to see that Invariants (i), (ii) and (iii) are satisfied in all three drawings.

So, assume that we have constructed the drawing Γ_f^{i-1} for G_f^{i-1} satisfying the invariants. G_f^i is obtained from G_f^{i-1} by adding a star with center w_i, leafs $x_1, \dots, x_k$, and such that

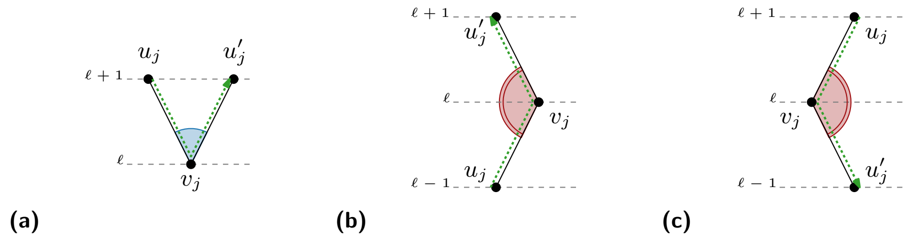

Figure 18 The boundary path $P_j = u_j, w_j, u'_j$ forms a (a) small angle, (b-c) a large angle in Γ^i_f. The boundary path is drawn green; horizontal dashed lines indicate levels.

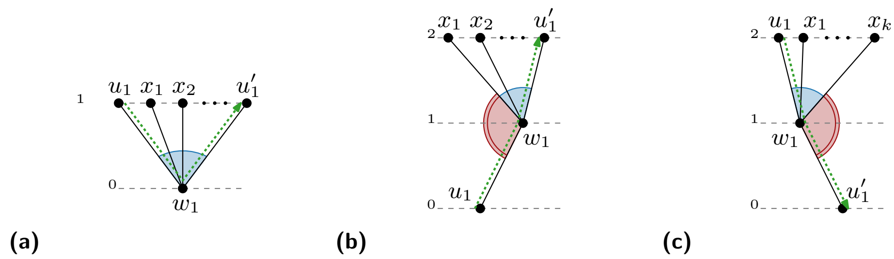

Figure 19 Possible drawings for G^1_f.

w_i is connected to the endpoints of the boundary path P_i of f_i. By construction, the new vertices are added in the exterior of Γ^{i-1}_f, satisfying Invariant (ii).

We consider two cases depending on whether P_i forms a small or a large angle in Γ^{i-1}_f. In the first case, let $\ell = \ell(u_i) = \ell(u'_i)$. We place w_i at level $\ell + 1$ and vertices $x_1, \ldots, x_k$ at level $\ell + 2$. In the constructed drawing the newly added vertices are placed at levels different from level 0, satisfying Invariant (i), while the new boundary paths (u_i, w_i, x_1) and (x_k, w_i, u'_i) form large angles and all other form small angles, satisfying Invariant (iii); see Figure 20a. Note that in the case where $k = 0$, that is there are no child vertices inside f_i, the only vertex of G_f inside f_i is vertex w_i, and no new boundary paths are created. In the second case, let ℓ be the level of vertex v_i. We place w_i at level ℓ and vertices $x_1, \ldots, x_k$ at level $\ell + 1$; refer to Figures 20b and 20c. The newly added vertices are placed at layers different from level 0, while (u_i, w_i, x_1) or (x_k, w_i, u'_i) forms a large angle, and all other new boundary paths form small angles. Therefore Invariants (i) and (iii) are satisfied in this case as well. Therefore, the constructed drawing of G_f satisfies Invariant (i) and the claim follows. $\lhd$

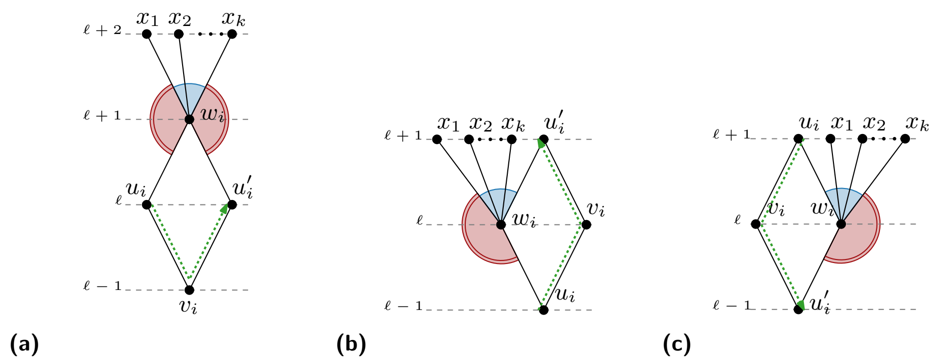

Figure 20 Extending Γ^{i-1}_f to Γ^i_f, when P_i forms a (a) small angle, or (b)–(c) a large angle.

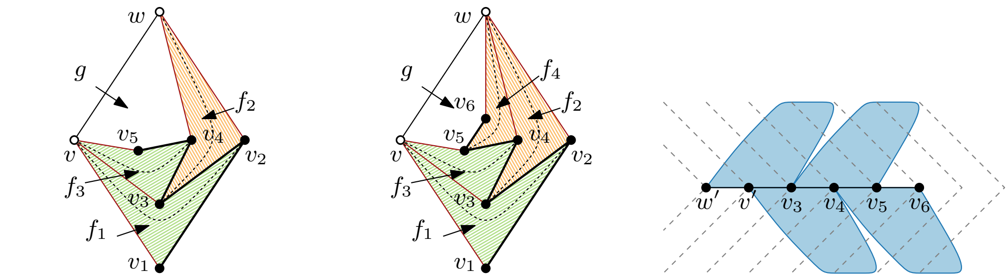

(a) $s = 3$ **(b)** $s = 4$ **(c)**

Figure 21 (a-b) Splitting a $[0, 0, 1, 1]$-face $f$into a series of [0,1,1,1]-faces (highlighted in green and orange) and an empty $[0, 0, 1, 1]$-face, (c) Schematic representations of Γ_f.

Figure 17 illustrates a schematic representation of different leveled planar drawings of G_f induced by the layer value-1 vertices of a [0,1,1,1]-face f, depending of the initial placement of vertices v', w and w'. Now we turn our attention to faces of type $[0, 0, 1, 1]$. We will prove that such a face can be split into an empty $[0, 0, 1, 1]$-face and a series of [0,1,1,1]-faces.

▷ Claim 26. Let $f = v, w, v', w'$ be a $[0, 0, 1, 1]$-face. There exists a path $(v_1, v_2, \ldots, v_{s+2})$ of $s + 2$ layer value-1 vertices ($s \geqslant 0$), such that the following hold:

- $v_1 = w'$ and $v_2 = v'$.
- Vertex v_i is adjacent to v (w) for odd (even, resp.) i, $1 \leqslant i \leqslant s + 2$.
- Face f is split into s faces $\{f_i\}_{1 \leqslant i \leqslant s}$ of type [0,1,1,1] and one empty $[0, 0, 1, 1]$-face g, where:
  - $f_{2j} = (w, v_{2j+2}, v_{2j+1}, v_{2j})$, for $1 \leqslant j \leqslant s/2$,
  - $f_{2j-1} = (v, v_{2j-1}, v_{2j}, v_{2j+1})$, for $1 \leqslant j \leqslant (s + 1)/2$, and
  - $g = (v, w, v_{s+2}, v_{s+1})$, if s is even, or $g = (w, v, v_{s+2}, v_{s+1})$ if s is odd.

Proof. Let $v_1 = w'$ and $v_2 = v'$. We will prove the claim using induction on the number k of layer value-1 vertices inside f. If f contains no layer value-1 vertices (that is $k = 0$ and f is empty), then $s = 0$ and the claim holds with $g = f$. Assume that the claim holds for $k' < k$ layer value-1 vertices and that f contains k layer value-1 vertices. Then, vertex u_1 of Figure 16d (which has layer value 1) exists and is a child inside f with parents v and v'. We let $v_3 = u_1$. Now f is split into face $f_1 = (v, v_1, v_2, v_3)$ which is of type [0,1,1,1], and the $[0, 0, 1, 1]$-face $g_1 = (w, v, v_3, v_2)$. As g_1 contains at most $k-1$ layer value-1 vertices, g_1 contains a path $(v'_1, \ldots, v'_{s'+2})$ of layer value-1 vertices that split g_1 into s' [0,1,1,1]-faces f'_i ($i = 1, \ldots, s'$) and an empty $[0, 0, 1, 1]$-face g' that satisfy the claim. For convenience, let $g_1 = (v'', w'', v'_2, v'_1)$, where $v'' = w$, $w'' = v$, $v'_2 = v_3$ and $v'_1 = v_2$. We set $v_{i+1} = v'_i$, for $i = 1, \ldots, s'+2$ and we will prove that the path $v_1, \ldots v_{s'+3}$ satisfies the properties of the claim. By definition, we have that $v_1 = w'$ and $v_2 = v'$. Also, in g_1, vertex v'_i is connected to v'' if i is odd and to w'' if i is even. Hence $v_j = v'_{j-1}$ is connected to $w = v''$ when j is even and to $v = w''$ when j is odd, as required. For the faces we have that $f_1 = (v, v_1, v_2, v_3)$, and we set $f_{i+1} = f'_i$, $i = 1, \ldots, s'$, and $g = g'$. We have that $f_{2j} = f'_{2j-1} = (v'', v'_{2j-1}, v'_{2j}, v'_{2j+1}) = (w, v_{2j}, v_{2j+1}, v_{2j+2})$ and $f_{2j-1} = f'_{2j-2} = (w'', v'_{2j}, v'_{2j-1}, v'_{2j-2}) = (v, v_{2j+1}, v_{2j}, v_{2j-1})$. On the other hand, as $s = s' + 1$, $g = g' = (w'', v'', v'_{s'+2}, v'_{s'+1}) = (v, w, v_{s+2}, v_{s+1})$, if s' is odd and s even, and $g = g' = (v'', w'', v'_{s'+2}, v'_{s'+1}) = (w, v, v_{s+2}, v_{s+1})$ if s' is even and s is odd. Hence the conditions of the claim hold. An example for $s = 3$ and $s = 4$ is shown in Figures 21a and 21b. ◁

In the following we compute a leveled planar drawing of a $[0, 0, 1, 1]$-face.

▷ Claim 27. The subgraph G_f of a $[0,0,1,1]$-face $f = v, w, v', w'$ has a leveled planar drawing such that level 0 contains only vertex w'; see Figure 21c.

Proof. For every face f_i ($i \geqslant 1$) of Claim 26, we create a leveled planar drawing Γ_i using Claim 25, such that Γ_i has only vertex v_i on level $i-1$ using the drawings of Figures 17b and 17c for odd and even i, respectively. On each level ℓ the vertices are ordered as follows. Vertices of the same face f_i (that are on level ℓ) appear consecutively. For $i \neq j \geqslant 1$, let u_i be a vertex inside face f_i and u_j a vertex inside f_j. If i is odd and j is even, then u_i appears before u_j along ℓ (from left to right); if both i and j are odd (even) with $i < j$, then u_i precedes (follows, resp.) u_j. Note that the derived drawing has only vertex w' on level 0 as claimed. ◁

Next, we focus on faces of type $[1,0,1,0]$. As the only layer value-1 vertices inside such faces belong to [0,1,1,1]-faces, we have the following.

▷ Claim 28. The subgraph G_f of a $[1,0,1,0]$-face $f = v, w, v', w'$ has a leveled planar drawing such that level 0 contains only vertices v and v', vertices of the [0,1,1,1]-face w, v, u_1, v' are drawn on levels above level 0, while vertices of the [0,1,1,1]-face w', v, u_k, v' are drawn on levels below level 0. In the special case where $u_1 = u_k$, then also u_1 is on level 0; see Figure 22.

Proof. We draw the [0,1,1,1]-face (w, v, u_1, v') using Claim 25 and such that vertex u_1 is the only vertex at level 1 (or 0 if $u_1 = u_k$) and all other vertices are at levels greater than 1 (or 0, resp.), as in Figure 17a. Similarly for face (w', v, u_k, v') we create a leveled planar drawing with u_k at level -1 (or 0 if $u_1 = u_k$) and all other vertices at levels below -1 (or 0, resp.). Vertices v and v' are placed at level 0 as shown in Figure 22a, if $u_1 \neq u_k$, otherwise they are placed together with $u_1 = u_k$ and such that u_1 is between v and v'; see Figure 22b. ◁

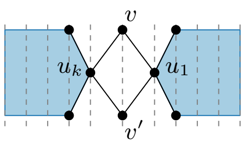

(a)

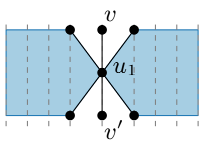

(b)

Figure 22 Schematic representations of Γ_f when f is a $[1,0,1,0]$-face with (a) $u_1 \neq u_k$ and (b) $u_1 = u_k$.

For a face f of type [0,0,1,0], recall that it consists of three faces; face (w, v, u_1, v'), which is of type $[0,0,1,1]$, face (v, u_1, v', u_k) of type [0,1,1,1] and face (w', v, u_k, v') of type $[0,0,1,1]$.

▷ Claim 29. The subgraph G_f of a [0,0,1,0]-face $f = v, w, v', w'$ has a leveled planar drawing such that level 0 contains only vertex v'; see Figure 23.

Proof. We use Claim 27 to produce a leveled planar drawing of face (w, v, u_1, v') with vertex v' on level 0 as shown in Figure 21c. A similar drawing is obtained for (w', v, u_k, v') with v' on level 0. Now face (v, u_1, v', u_k) is drawn as in Figure 17a with v' on level 0, using Claim 25. The three drawings can be glued together as depicted in Figure 23a, or Figure 23b depending on whether $u_1 \neq u_k$ or $u_1 = u_k$ (in which case the $[0,1,1,1]$-face (v, u_1, v', u_k) does not exist). ◁

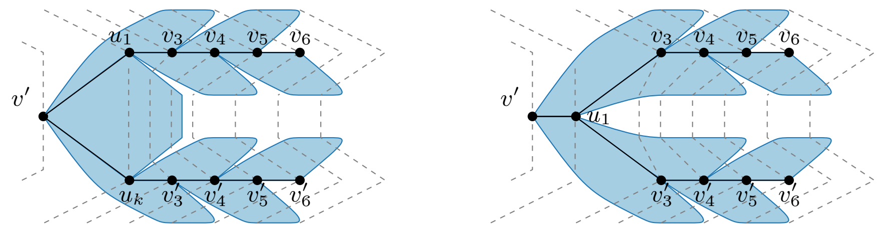

(a) **(b)**

Figure 23 Schematic representations of Γ_f when f is a [0,0,1,0]-face with (a) $u_1 \neq u_k$ and (b) $u_1 = u_k$.

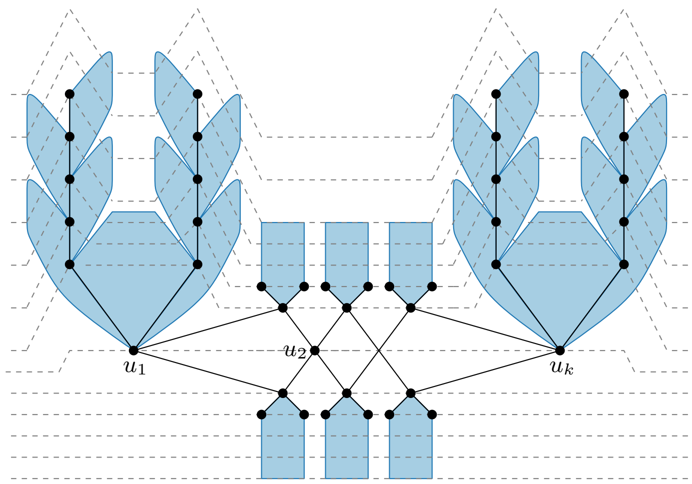

Figure 24 Schematic representations of Γ_f when f is a $[0, 0, 0, 0]$-face.

The only type of faces that we have not considered yet are $[0, 0, 0, 0]$-faces. We combine leveled planar drawings for faces (w, v, u_1, v'), (w', v, u_k, v') and faces $f_i = (u_i, v, u_{i+1}, v')$ for $i = 1, \ldots, k-1$. We create drawings for the [0,0,1,0]-faces (w, v, u_1, v') and (w', v, u_k, v') using Claim 29, such that u_1 and u_k are the only vertices placed at level 0. Then for every face f_i $(i = 1, \ldots, k-1)$, we use Claim 28; vertices u_i, for $i = 1, \ldots, k$ are placed at level 0. We combine the drawings as shown in Figure 24, by ordering the vertices on each level as follows. Vertices at level ℓ that belong to the same face appear consecutively along ℓ. Vertices of face (w, v, u_1, v'), precede all vertices of faces f_i for $i = 1, \ldots, k-1$, and vertices of (w', v, u_k, v') appear last along ℓ. For two faces f_i and f_j with $1 \leqslant i < j \leqslant k-1$, we have that vertices of f_i precede vertices of f_j.

So far, we focused on a $[0, 0, 0, 0]$ face f and determined a leveled planar drawing of G_f, which is the subgraph induced by vertices of level 1 inside f. Clearly, starting from any face with all vertices having the same layer value λ, we can compute a leveled planar drawing of the layer value-$(\lambda + 1)$ subgraph of G that is inside this face. Now we are ready to compute the tree-partition of a 2-generate quadrangulation G. We assign layer value equal to 0 to the vertices on the outer face of G, and compute the layer value of all other vertices. Let G_λ denote the subgraph of G induced by vertices of layer value λ $(\lambda \geqslant 0)$. We have that all edges of G are either level edges (that is, belong to G_λ for some value of λ), or connect subgraphs of consecutive layer values λ and $\lambda + 1$. In particular, each connected component $H_{\lambda+1}$ of $G_{\lambda+1}$ is located inside a 4-face $f(H_{\lambda+1})$ of G_λ, and the vertices of $f(H_{\lambda+1})$ are the only vertices of G_λ that are connected to the vertices of that connected component of

$H_{\lambda+1}$. Now, for each value of λ, we put the connected components of G_λ into separate bags, and therefore each bag contains a leveled planar graph. For a bag that contains connected component H_λ, we define its parent to be the bag that contains the component where $f(H_\lambda)$ belongs to. As each connected component H_λ lies in the interior of a single face $f(H_\lambda)$, the defined bags create a tree T with root-bag consisting of the outer vertices of G (with layer value 0). Additionally, the shadow of each bag consists of at most four vertices, and therefore the shadow width of T is at most 4. The lemma follows. ◂

▸ **Theorem 6.** *Every 2-degenerate quadrangulation admits a 5-queue layout.*

Proof. Combine Lemma 24 with Lemma 23. Observe that *every* leveled planar graph admits a 1-queue layout in which the faces are nicely ordered with respect to the layout. That implies that we can apply Lemma 23 with $q = 1$ (the queue number of the bags) and $k = 4$ (the shadow width of the tree-partition). ◂

6 Open Questions

In this work, we focused on the queue number of bipartite planar graphs and related subfamilies. Next we highlight a few questions for future work.

- First, there is still a significant gap between our lower and upper bounds for the queue number of bipartite planar graphs.
- Second, although 2-degenerate quadrangulations always admit 5-queue layouts, the question of determining their exact queue number remains open.
- Third, for stacked quadrangulations, our upper bound relies on the strong product theorem. We believe that a similar approach as for 2-degenerate quadrangulations could lead to a significant improvement.
- Perhaps the most intriguing questions are related to mixed linear layouts of bipartite planar graphs: One may ask what is the minimum q so that each bipartite planar graph admits a 1-stack q-queue layout.
- Finally, the recognition of 1-stack 1-queue graphs remains an important open problem even for bipartite planar graphs.

References

1 Alam, J.M., Bekos, M.A., Gronemann, M., Kaufmann, M., Pupyrev, S.: Lazy queue layouts of posets. In: Auber, D., Valtr, P. (eds.) Graph Drawing and Network Visualization 2020. Lecture Notes in Computer Science, vol. 12590, pp. 55–68. Springer (2020). https://doi.org/10.1007/978-3-030-68766-3_5

2 Alam, J.M., Bekos, M.A., Gronemann, M., Kaufmann, M., Pupyrev, S.: Queue layouts of planar 3-trees. Algorithmica pp. 1–22 (2020). https://doi.org/10.1007/s00453-020-00697-4

3 Angelini, P., Bekos, M.A., Kindermann, P., Mchedlidze, T.: On mixed linear layouts of series-parallel graphs. Theor. Comput. Sci. **936**, 129–138 (2022). https://doi.org/10.1016/j.tcs.2022.09.019

4 Auer, C., Gleißner, A.: Characterizations of deque and queue graphs. In: Kolman, P., Kratochvíl, J. (eds.) Graph-Theoretic Concepts in Computer Science. pp. 35–46. Springer Berlin Heidelberg, Berlin, Heidelberg (2011)

5 Bannister, M.J., Devanny, W.E., Dujmović, V., Eppstein, D., Wood, D.R.: Track layouts, layered path decompositions, and leveled planarity. Algorithmica **81**(4), 1561–1583 (2019). https://doi.org/10.1007/s00453-018-0487-5

6 Battista, G.D., Frati, F., Pach, J.: On the queue number of planar graphs. SIAM J. Comput. **42**(6), 2243–2285 (2013). https://doi.org/10.1137/130908051

7 Bekos, M., Gronemann, M., Raftopoulou, C.N.: An improved upper bound on the queue number of planar graphs. Algorithmica pp. 1–19 (2022). https://doi.org/10.1007/s00453-022-01037-4

8 Bekos, M.A., Bruckdorfer, T., Kaufmann, M., Raftopoulou, C.N.: The book thickness of 1-planar graphs is constant. Algorithmica **79**(2), 444–465 (2017). https://doi.org/10.1007/s00453-016-0203-2

9 Bekos, M.A., Da Lozzo, G., Hlinený, P., Kaufmann, M.: Graph product structure for h-framed graphs. CoRR **abs/2204.11495** (2022). https://doi.org/10.48550/arXiv.2204.11495

10 Bekos, M.A., Förster, H., Gronemann, M., Mchedlidze, T., Montecchiani, F., Raftopoulou, C.N., Ueckerdt, T.: Planar graphs of bounded degree have bounded queue number. SIAM J. Comput. **48**(5), 1487–1502 (2019). https://doi.org/10.1137/19M125340X

11 Bekos, M.A., Kaufmann, M., Klute, F., Pupyrev, S., Raftopoulou, C.N., Ueckerdt, T.: Four pages are indeed necessary for planar graphs. J. Comput. Geom. **11**(1), 332–353 (2020). https://doi.org/10.20382/jocg.v11i1a12

12 Bernhart, F., Kainen, P.C.: The book thickness of a graph. J. Comb. Theory, Ser. B **27**(3), 320–331 (1979). https://doi.org/10.1016/0095-8956(79)90021-2

13 Bhore, S., Ganian, R., Montecchiani, F., Nöllenburg, M.: Parameterized algorithms for queue layouts. J. Graph Algorithms Appl. **26**(3), 335–352 (2022). https://doi.org/10.7155/jgaa.00597

14 Biedl, T.C., Shermer, T.C., Whitesides, S., Wismath, S.K.: Bounds for orthogonal 3D graph drawing. J. Graph Algorithms Appl. **3**(4), 63–79 (1999). https://doi.org/10.7155/jgaa.00018

15 Bose, P., Morin, P., Odak, S.: An optimal algorithm for product structure in planar graphs. In: Czumaj, A., Xin, Q. (eds.) SWAT 2022. LIPIcs, vol. 227, pp. 19:1–19:14. Schloss Dagstuhl - Leibniz-Zentrum für Informatik (2022). https://doi.org/10.4230/LIPIcs.SWAT.2022.19

16 Campbell, R., Clinch, K., Distel, M., Gollin, J.P., Hendrey, K., Hickingbotham, R., Huynh, T., Illingworth, F., Tamitegama, Y., Tan, J., Wood, D.R.: Product structure of graph classes with bounded treewidth. CoRR **abs/2206.02395** (2022). https://doi.org/10.48550/arXiv.2206.02395

17 Chung, F.R.K., Leighton, F.T., Rosenberg, A.L.: Embedding graphs in books: A layout problem with applications to VLSI design. SIAM Journal on Algebraic and Discrete Methods **8**(1), 33–58 (1987)

18 de Col, P., Klute, F., Nöllenburg, M.: Mixed linear layouts: Complexity, heuristics, and experiments. In: Archambault, D., Tóth, C.D. (eds.) Graph Drawing and Network Visualization. pp. 460–467. Springer International Publishing, Cham (2019). https://doi.org/10.1007/978-3-030-35802-0_35

19 Dujmovic, V., Eppstein, D., Hickingbotham, R., Morin, P., Wood, D.R.: Stack-number is not bounded by queue-number. Comb. **42**(2), 151–164 (2022). https://doi.org/10.1007/s00493-021-4585-7

20 Dujmović, V., Frati, F.: Stack and queue layouts via layered separators. J. Graph Algorithms Appl. **22**(1), 89–99 (2018). https://doi.org/10.7155/jgaa.00454

21 Dujmović, V., Joret, G., Micek, P., Morin, P., Ueckerdt, T., Wood, D.R.: Planar graphs have bounded queue-number. Journal of the ACM (JACM) **67**(4), 1–38 (2020). https://doi.org/10.1145/3385731

22 Dujmović, V., Morin, P., Wood, D.R.: Layout of graphs with bounded tree-width. SIAM Journal on Computing **34**(3), 553–579 (2005). https://doi.org/10.1137/S0097539702416141

23 Dujmovic, V., Pór, A., Wood, D.R.: Track layouts of graphs. Discret. Math. Theor. Comput. Sci. **6**(2), 497–522 (2004)

24 Dujmovic, V., Wood, D.R.: Three-dimensional grid drawings with sub-quadratic volume. In: Liotta, G. (ed.) Graph Drawing 2003. Lecture Notes in Computer Science, vol. 2912, pp. 190–201. Springer (2003). https://doi.org/10.1007/978-3-540-24595-7_18

25 Felsner, S., Huemer, C., Kappes, S., Orden, D.: Binary labelings for plane quadrangulations and their relatives. Discret. Math. Theor. Comput. Sci. **12**(3), 115–138 (2010)

26 Heath, L.S., Leighton, F.T., Rosenberg, A.L.: Comparing queues and stacks as mechanisms for laying out graphs. SIAM J. Discret. Math. **5**(3), 398–412 (1992). https://doi.org/10.1137/0405031

27 Heath, L.S., Rosenberg, A.L.: Laying out graphs using queues. SIAM Journal on Computing **21**(5), 927–958 (1992). https://doi.org/10.1137/0221055

28 Merker, L., Ueckerdt, T.: The local queue number of graphs with bounded treewidth. In: Auber, D., Valtr, P. (eds.) Graph Drawing and Network Visualization 2020. Lecture Notes in Computer Science, vol. 12590, pp. 26–39. Springer (2020). https://doi.org/10.1007/978-3-030-68766-3_3

29 Morin, P.: A fast algorithm for the product structure of planar graphs. Algorithmica **83**(5), 1544–1558 (2021). https://doi.org/10.1007/s00453-020-00793-5

30 Pupyrev, S.: A SAT-based solver for constructing optimal linear layouts of graphs, source code available at `https://github.com/spupyrev/bob`

31 Pupyrev, S.: Mixed linear layouts of planar graphs. In: Frati, F., Ma, K.L. (eds.) Graph Drawing and Network Visualization. pp. 197–209. Springer International Publishing, Cham (2018). https://doi.org/10.1007/978-3-319-73915-1_17

32 Pupyrev, S.: Improved bounds for track numbers of planar graphs. Journal of Graph Algorithms and Applications **24**(3), 323–341 (2020). https://doi.org/10.7155/jgaa.00536

33 Ueckerdt, T., Wood, D.R., Yi, W.: An improved planar graph product structure theorem. Electron. J. Comb. **29**(2) (2022). https://doi.org/10.37236/10614

34 Wiechert, V.: On the queue-number of graphs with bounded tree-width. Electr. J. Comb. **24**(1), P1.65 (2017). https://doi.org/10.37236/6429

35 Wood, D.R.: Product structure of graph classes with strongly sublinear separators. CoRR **abs/2208.10074** (2022). https://doi.org/10.48550/arXiv.2208.10074

36 Yannakakis, M.: Embedding planar graphs in four pages. J. Comput. Syst. Sci. **38**(1), 36–67 (1989). https://doi.org/10.1016/0022-0000(89)90032-9

37 Yannakakis, M.: Planar graphs that need four pages. J. Comb. Theory, Ser. B **145**, 241–263 (2020). https://doi.org/10.1016/j.jctb.2020.05.008